BULLETIN OF BIOTECHNOLOGY

e-ISSN: 2717-8323

Cilt: 3 Volume: 2 Year: 2022

BULLETIN OF BIOTECHNOLOGY

Cilt: 3 Volume: 2 Year: 2022

Published Biannually

Corresponding Address
Karamanoğlu Mehmetbey University, Faculty of Health, Sciences, Department of Nutrition and Dietetics, Karaman, Turkey
E-mail: mtdogan1@gmail.com
Web: https://www.dergipark.org.tr/biotech

Owner / Publisher
Assist. Prof. Dr. Muhammet DOĞAN
This journal is peer-reviewed and published twice (June, December) a year.

e-ISSN 2717-8323

BULLETIN OF BIOTECHNOLOGY

e-ISSN 2717-8323

Cilt: 3 Volume: 2 Year: 2022

Contents

RESEARCH ARTICLE
Bull Biotechnol (2022) 3(2):27-31
https://doi.org/10.51539/biotech.1110858 Jurnal homepage:www.dergipark.org.tr/biotech

Bulletin of Biotechnology

A Molecular Docking Approach to Evaluate the Pharmacological Properties of 1-(4-amino-1,2,5-oxadiazol-3-yl)-N'-(1-(3-hydroxyphenyl)vinyl)-5-(thiophen-2-yl)1H-1,2,3-triazole-4-carbohydrazide Treatment Candidate for Use against COVID-19

Mohamed A.M.A Abasher *

* *Department of Biochemistry, Faculty of Medical .L.S, Dongola University, Sudan*.

*Corresponding author : mo11mmed@yahoo.com
Orcid No: https://orcid.org/ 0000-0002-2891-6593

Received : 29/04/2022
Accepted : 21/12/2022

Abstract: Abstract: In recent years, the new Coronavirus known as COVID-19 has caused a pandemic that has caused severe health problems. The virus is spreading rapidly worldwide, and finding potential antiviral drugs that can inhibit virus proteins is crucial. Recently, CoVID-19 crystal structure elucidated such as major protease Mpro (PDB: 6LU7), SARS-CoV- main peptidase (2GTB), human ACE2 (PDB: 1O86), human coronavirus papain-like proteases (PDB: 4OW0) SARS-Coronavirus NSP12 protein (PDB: 6NUR), COVID-19 main protease (PDB:6lu7). These proteins are essential for virus replication, so they are potential targets for CoVID-19 drugs. In this study, we used the molecular docking models to study the binding interactions between anodyne called 1-(4-amino-1,2,5-oxadiazol-3-yl)-N'-(1-(3-hydroxyphenyl)vinyl)-5-(thiophen-2-yl)-1H-1,2,3-triazole-4-carbohydrazide(Zinc ID 000002613203) using MOE 2015.10. It has been observed Obtained results by molecular docking showed that a stronger bond and high affinity with 4OW0 -8.1949, 6lu7 -7.7925, 1O86-7.5757, -6.7832 -7.4101, 2GTB -7.2510 kcal/mol). Based on the binding energy score, this compound are suitable for testing against Coronavirus and could be considered potential inhibitor of COVID-19 infection.)

Keywords: Anti-viral effects; Molecular docking; MOE; COVID-19

1 Introduction

The recent outbreak of the deadly coronavirus pandemic (COVID -19) has raised severe global health concerns. Viruses are spreading rapidly in the current situation.

Since its emergence in late December 2019 in China, the number of confirmed cases is 464,809,377, including 6,062,536 deaths worldwide, and the number of infections continues to increase (WHO Coronavirus (COVID-19) Dashboard, 2022). Due to The absence of approved medications, new therapeutic molecules must be discovered (Gurung et al. 2021).

Drug development of a new drug usually takes more than ten years (Songet al. 2009). Even with the high investment and time required to discover new medicines, less than 14% of clinical trials are successful (Zhong et al. 2018,Gurung et al. 2021). The cost of bringing a medication to market can be up to 2 billion USD(DiMasiet al. 2016).

Computer simulations have aided in accelerating the discovery and development of new medications and drugs by reducing costs and time (Gurung et al., 2021). Molecular docking is commonly employed to study silico binding between proteins and ligands to prioritize compounds and identify new lead medication compounds. This could be a helpful tool for developing and discovering new potential antiviral inhibitors against SARS-CoV-2 (Serafim et al. 2021).

Nowadays, molecular docking programs are widely and routinely used in computational drug discovery, mainly in virtual library screening campaigns (VS). (Jorgensen 2004). The first step of structure-based drug discovery (SBDD) is to identify the drug ligand that best fits the binding pocket of the target protein. This method was developed to predict the geometry of binding complexes between proteins and ligands (Kuntz et al. 1982,Gioia et al. 2017).

Our study aims to find an effective drug candidate (Anodyne Zinc ID 2613203) against COVID -19, targeting the proteins 2GTB and 6LU7 and 1O86 and 6NUR, and 4OW0 and the major protease of COVID -19 by using A Computer simulations methods.

2 Materials and Method

All docking experiments were used MOE 2015.10 for the analysis. The simulation was performed on a high-performance computer .

2.1. Preparation of Ligand

Ligand structures were retrieved from the Zinc database (http://zinc.docking.org). Smiles were used to load the structures into MOE and with the partial charges added. For docking purposes, structures were reduced and stored as a database. (Adebambo 2020).

2.2. Preparation of Proteins

Crystal structure of 2GTB and 6LU7 and 1O86 and 6NUR and 4OW0 proteins was retrieved from the Protein Data Bank (http://www.rcsb.org) with 2.16 Å, 2.00 Å, 2.16 Å, 2.00 Å, 2.10 Å, 3.10 resolution respectively.

The structure of the protein was refined by removing ligands and water molecules already bound to it. and protein preparation by, 3D protonation was performed in MOE. to remove defects after correcting, The binding site of the protein was found using MOE software's site finder.

2.3. Molecular docking

Using MOE docking tool, was accomplished to docking the substance anodyne (Zinc ID 2613203) to the allosteric ligand binding site of 2GTB and 6LU7 and 1O86 and 6NUR and 4OW0 proteins. The potential binding pocket was identified using the Site Finder Tool from MOE and then subjected to a docking process. Using a London dG scoring function, the top five docked poses were identified. The docking process was refined by applying a force field algorithm that kept the receptor rigid. Based on the root mean square deviation (RMSD), measured in angstroms (Å), and the docking score, the best interacting ligands and molecules were selected.

Previously reported co-crystallized ligand. Ligand-receptor binding analysis was performed using the LigX tool in MOE. The system visualizes potential residues interacting with ligand molecules using 2D images representing the forces stabilizing the ligand molecules in the binding pockets of the receptor (Khan et al. 2017).

3 Results

In the present study, virtual screening of the (Anodyne Zinc ID 2613203) substance (Figure 1) against 2GTB and 6LU7 and 1O86 and 40W0 6NUR .Where these proteins have been presented as attractive drug targets.(Pires et al., 2015,Dainaet al. 2017)

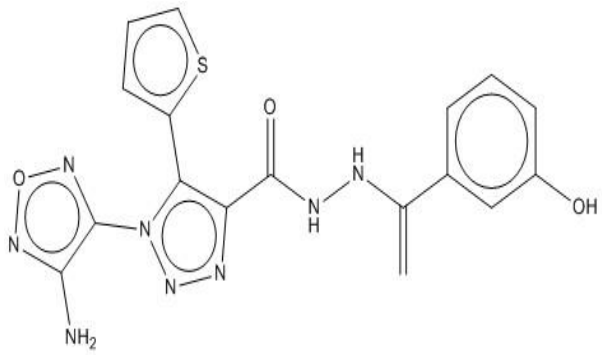

Fig. 1 Structure of Anodyne Zinc ID 2613203 substance

Docking studies were performed using the Molecular Operating Environment (MOE 2015.10). The results of these experiments showed strong interactions of the potential compound candidates anodyne Zinc ID 2613203 substance against the COVID -19 major protease (PDB:6lu7) and SARS-CoV major peptidase (PDB: 2GTB) and 1O86 and 40W0, 6NUR. After the successful docking of these compounds to the COVID -19 target proteins mentioned above, different modes of ligand-protein interactions with a specific docking score (binding energy) are generated. Binding modes with the lowest binding energies are considered the best binding modes since they are the most stable for the ligand. The observed binding energy results are summarized in Table 1,2,3,4,5.

Based on the molecular docking result, Anodyne Zinc ID 2613203 substances could be useful in treating infected patients. We find that the docking score reaches -8.1949 in 40W0, -7.2510 in 2GTB, -7.5757 in 1O86, -6.7832 in 6NUR, and -7.7925 in 6lu7.

The interaction of specific amino acids involved in ligand-protein interactions was also recorded. Followingthemolecular docking results, the 2-dimensional visualization results of the ligand-residue interactions showed that the (Anodyne Zinc ID 2613203) substance

latches into the binding pocket in 1086 with four interactions; it has a hydrogen bonding interaction with Met223 in the binding site and three pi-Hydrogen interactions with different amino acids contained within the binding pocket, these a six-ring Ile204 pi-Hydrogen, a five-ring Lys118 pi-Hydrogen, and a five-ring Glu403 pi-H interaction. (Figure 2).

While the anodyne Zinc ID 2613203 substance compound is bound to the 2GTB protein, it has a total of four binding interactions with the amino acids in the binding pocket, showing that the drug molecule latches onto the binding pocket with four interactions, it has hydrogen bonding interactions with His in the binding site. And two pi-Hydrogen interactions with different amino acids within the binding pocket, these one five-ring Asn142 pi-Hydrogen, and one five-ring Glu166 pi-Hydrogen interaction (Figure 3).

The ligand interaction with the 4OW0 protein (Figure 4) showed that the Anodyne Zinc ID 2613203 latches into the binding pocket with four interactions. With the amino acids

in the binding pocket, it has one hydrogen bonding interaction with Asp165(A) in the binding site and three pi-Hydrogen interactions with different amino acids within the binding pocket, these one 5 ring Tyr(A) 269 and Gly(A)164 and Asp165(A) pi-Hydrogeninteraction.

As shown in Figure 5 below, the ligand occupied the binding pocket of the 6NUR protein, and the Anodyne had four hydrogen bonds with amino acids Ala-554 and Thr-556 present in the binding pocket, and two pi-Hydrogen interactions with different amino acids within the binding pocket, namely a 6-ring Arg624 pi-Hydrogen and a 5-ring Arg553 pi-Hydrogen interaction.

The ligand interaction with 6LU7 protein (Figure 6) showed that the Anodyne Zinc ID 2613203 latches into the binding pocket with six interactions, the amino acids in the binding pocket interacting strongly with two Glu, two His, and one Cys amino acids. And two pi-Hydrogen interactions with different amino acids within the binding pocket, these Two 5-ring Gln(A) 189 and Gln189(B) pi-Hydrogen interactions.

Table 1. Interaction between drug candidate and 2GTB and their docking properties of the top five poses

no.	S	rmsd_ refine	E_conf	E_place	E_score1	E_refine
1	-7.2510	1.6070	88.2360	-89.8618	-12.3420	-38.9720
2	-7.0690	1.6012	82.5988	-56.8477	-10.2660	-40.0395
3	-6.8280	1.5127	74.0142	-83.6527	-9.9414	-42.3033
4	-6.7807	2.2541	79.3597	-92.3093	-10.8162	-40.2780
5	-6.7548	1.4512	73.7242	-106.0715	-11.2040	-41.5857

Table. 2. Interaction between drug candidate and 1086 and their docking properties of the top five poses .

no.	S	rmsd_ refine	E_conf	E_place	E_score1	E_refine
1	-7.5757	1.0870	76.0101	-87.7858	-10.7714	-44.6827
2	-7.2876	1.8361	80.5905	-105.1578	-10.2660	-40.7860
3	-7.1614	1.3610	79.0984	-101.0885	-10.3269	-38.9334
4	-7.0618	2.1344	82.5177	-65.1269	-9.9578	-41.7902
5	-7.0274	1.4959	84.4009	-90.1260	-11.3677	-39.2677

Table. 3. Interaction between drug candidate and 40W0 and their docking properties of the top five poses .

no.	S	rmsd_ refine	E_conf	E_place	E_score1	E_refine
1	-8.1949	1.7178	80.0550	-104.5792	-11.1493	-48.3560
2	-8.1541	1.2627	74.4491	-81.7984	-11.4903	-48.0648
3	-8.0749	2.2633	76.6276	-89.0673	-11.6562	-46.2307
4	-7.6948	1.7017	74.5244	-73.9517	-11.5709	-44.6842
5	-7.6351	1.4096	76.8360	-109.5280	-11.2194	-43.7298

Table. 4. Interaction between drug candidate and 6NUR and their docking properties of the top five poses .

no.	S	rmsd_ refine	E_conf	E_place	E_score1	E_refine
1	-7.4101	2.2200	79.3847	-70.9006	-10.4089	-45.2058
2	-6.8108	3.5918	79.8446	-70.7154	-10.5112	-34.4157
3	-6.7832	1.0721	75.0903	-80.0705	-10.1899	-35.9292
4	-6.5244	1.4898	76.9420	-97.5033	-11.6161	-36.2727
5	-6.5037	1.5257	75.0589	-76.7025	-10.2171	-32.9803

Table. 5. Interaction between drug candidate and 6lU7 and their docking properties of the top five poses .

no.	S	rmsd_ refine	E_conf	E_place	E_score1	E_refine
1	-7.7925	1.5134	80.3739	-80.8232	-11.9235	-45.9976
2	-7.3862	1.5224	80.0461	-77.8064	-10.7242	-39.1877
3	-6.9489	1.1649	84.8352	-99.1665	-11.5751	-40.1935
4	-6.8982	2.4029	81.2241	-101.2040	-10.9526	-40.3345
5	-6.8760	1.7116	75.2210	-89.9736	-12.2249	-42.6265

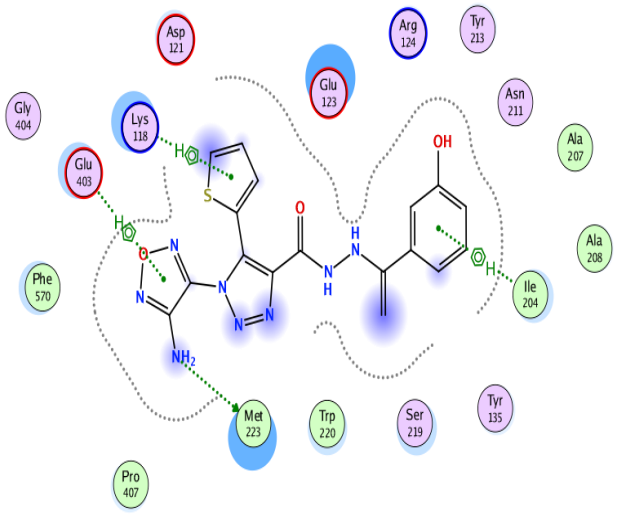

Figure 2 The interaction of Anodyne Zinc ID 2613203 substance with the amino acids in the binding pocket of 1086

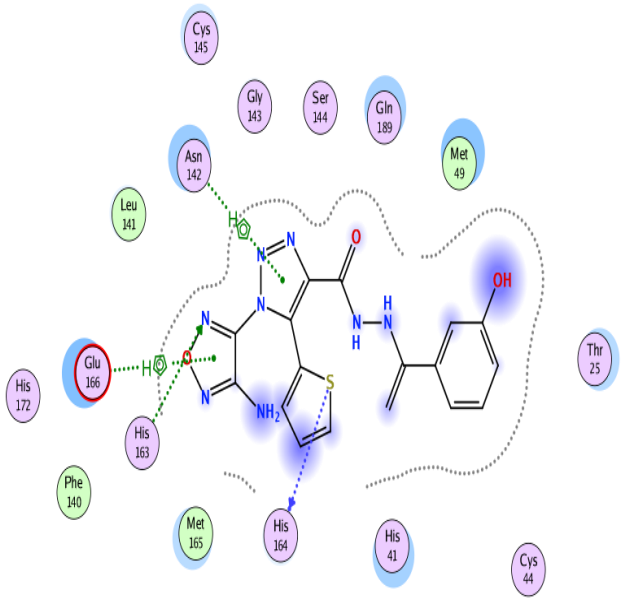

Figure 3. The interaction of Anodyne Zinc ID 2613203 substance with the amino acids in the binding pocket of 2GTB

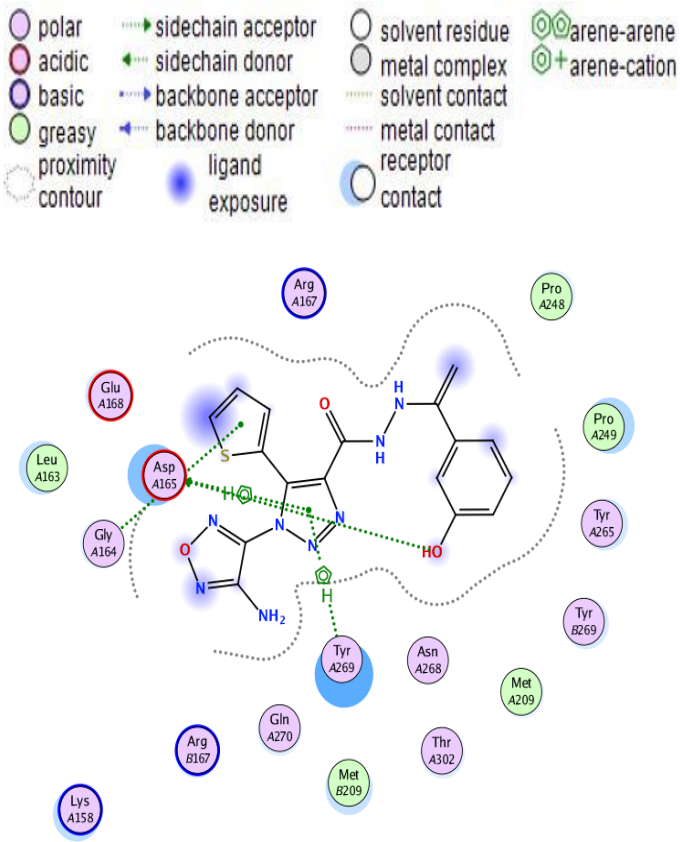

Figure 4. The interaction of Anodyne Zinc ID 2613203 substance with the amino acids in the binding pocket of 40W0

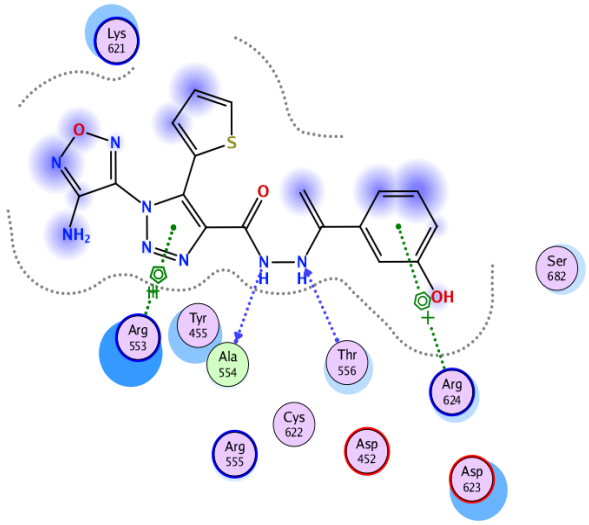

Figure 5. The interaction of Anodyne Zinc ID 2613203 substance with the amino acids in the binding pocket of 6NUR

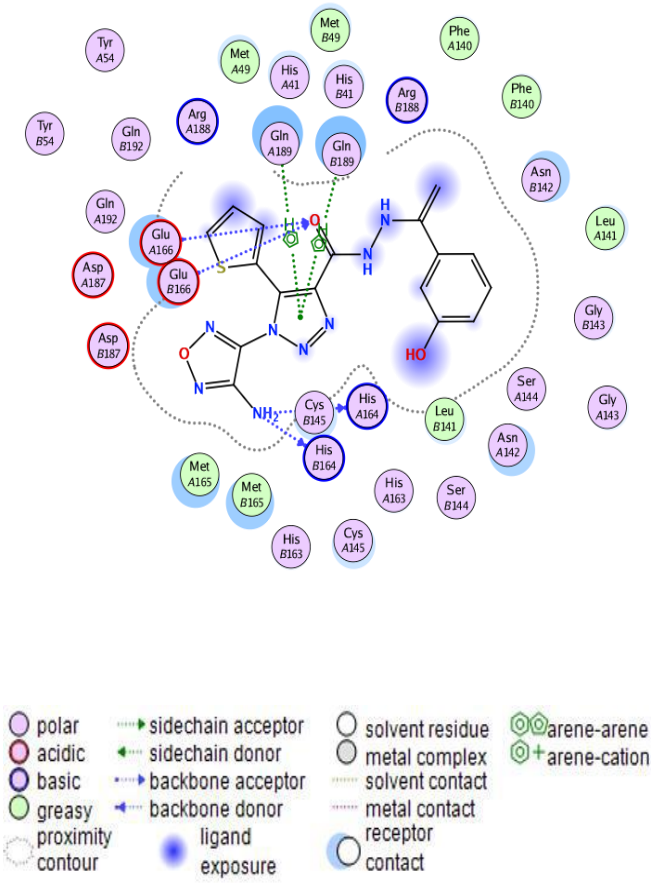

Figure 6. The interaction of Anodyne Zinc ID 2613203 substance with the amino acids in the binding pocket of 6Lu7.

4 Discussion

This study involves the In silico interactions of anodyne Zinc ID 2613203 substances. With int he proteins 4OW0, 6lu7, and 6NUR, 1O86, 2GTB, and 6NUR which play a role in virus entry into host cells and virus replication.

Based on the docking results, the ligands found potential inhibitory effects of 4OW0, 6lu7, and 6NUR, 1O86, 2GTB, 6NUR protein with binding energy (-8.1949, -7.7925, -7.5757, -7.4101, -7.2510 kcal/mol) when comparing the efficacy of anodyne Zinc ID 2613203 substances.

Comparison with other drugs used to treat covid-19 shows the compound chloroquine (-6.30 kcal/mol) and hydroxychloroquine (-7.28 kcal/mol) mentioned in the study.(Amin and Abbas 2020) atazanavir (-7.912) , Remdesvir (-7.804) , Amprenavir (-7.747) , Lopinavir -(7.041) , Nelfinavir (-6.73) , Oseltamivir (-5.825) , Tipranavir -(5.64) , Galidesvir (-4.967) kcal/mol (Kumar et al., 2020). The proposed compound has high docking scores.

The compound contains a sulphur atom in its composition. Sulphur is considered to be nucleophilic because its size makes it easy to polarize. S-atoms in compounds show H-bonding interactions with the catalytic residue His164 of 2GTB. In general, the Nitrogen groups in the aliphatic and cyclic structures of the substance form strong and dense H-bonds with the critical catalytic residues of 40W0, 6LU7, protein. In addition, there are hydrogen bonds and pi-Hydrogen interactions with various amino acids within the binding pocket in 1O86, 2GTB), 4OW0), 6NUR, and 6LU7. All these molecular interaction properties enhance the inhibition potential of anodyne Zinc ID 2613203 substance for CoVID-19.

5 Conclusion

Corona disease is still a major problem that should be solved by developing new bioactive agents. The appearance of new mutations leads to problems with drug resistance. This study addresses the in silico interactions of 1-(4-amino-1,2,5-oxadiazol-3-yl)-N'-(1-(3-hydroxyphenyl)vinyl)-5-(thiophen-2-yl)-1H-1,2,3-triazole-4-carbohydrazide with protein 4OW0, 6lu7, and 6NUR, 1O86, 2GTB, 6NUR, which plays a role in the method of virus entry into host cells and virus replication. Based on the docking results, the ligands found potential inhibitory effects of 4OW0, 6lu7, and 6NUR, 1O86, 2GTB, 6NUR protein with binding energy (-8.1949, -7.7925, -7.5757, -7.4101, -7.2510 kcal/mol). Suggesting that it is a potent candidate for further in vitro and in vivo studies as an experimental drug for use against Covid-19.

Acknowledgements

There was no specific source of funding, public, commercial, or nonprofit, for this research.

Conflict of interest:

The author declares that there are no conflicts of interest related to the publication of this article

References

Adebambo K(2020) Computational Investigation of the Interaction of Anti-Influenza Drugs with CoVID-19 Protein. CMB10(02): 45-60.

Amin M, Abbas G(2020)Docking study of chloroquine and hydroxychloroquine interaction with RNA binding domain of nucleocapsid phospho-protein–an in silico insight into the comparative efficacy of repurposing antiviral drugs. J Biomol StructDyn 1–13. doi:10.1080/07391102.2020.1775703

Covid19.who.int. (2022) WHO Coronavirus (COVID-19) Dashboard. [online] Available at. https://covid19.who.int .Accessed 21 March 2022

Daina A, MichielinO,Zoete V(2017) SwissADME: a free web tool to evaluate pharmacokinetics, drug-likeness and medicinal chemistry friendliness of small molecules. Sci Rep7(1).

DiMasi J, Grabowski H,HansenR(2016) Innovation in the pharmaceutical industry: New estimates of R&D costs. J Health Econ, 47: 20-33.

Gioia D, Bertazzo M, Recanatini M, Masetti M, Cavalli A(2017) Dynamic Docking: A Paradigm Shift in Computational Drug Discovery. Molecules 22(11): 2029.

Gurung A, Ali M, Lee J, Farah M, Al-Anazi K(2021) An Updated Review of Computer-Aided Drug Design and Its Application to COVID-19. BioMed Res Int 2021: 1-18.

JorgensenW(2004) The Many Roles of Computation in Drug Discovery. Science 303(5665): 1813-1818.

Khan W, Ashfaq UA, Aslam S, Saif S, Aslam T, Tusleem K, Maryam A, Tahir Ul (2017) Anticancer screening of medicinal plant phytochemicals against Cyclin-Dependent Kinase-2 (CDK2): An in-silico approach. ALS | www.als-journal.com (Vol. 4). www.als-journal.com

Kumar S, Sharma PP, Shankar U, Kumar D, Joshi SK, Pena L, Durvasula R, Kumar A, KempaiahP, Poonam, Rathi B (2020) Discovery of New Hydroxyethylamine Analogs against 3CLproProtein Target of SARS-CoV-2: Molecular Docking, Molecular Dynamics Simulation, and Structure-Activity Relationship Studies. J Chem Inf Model60(12): 5754–5770. doi:10.1021/ACS.JCIM.0C00326

Kuntz I, Blaney J, Oatley S, Langridge R,Ferrin T(1982)A geometric approach to macromolecule-ligand interactions. J Mol Biol161(2): 269-288.

Pires DE, BlundellTL, Ascher DB (2015) pkCSM: Predicting small-molecule pharmacokinetic and toxicity properties using graph-based signatures. J Med Chem 58(9): 4066–4072. doi:10.1021/acs.jmedchem.5b00104

Serafim M, Gertrudes J, Costa D, Oliveira P, MaltarolloV, Honorio K(2021) Knowing and combating the enemy: a brief review on SARS-CoV-2 and computational approaches applied to the discovery of drug candidates. Biosci Rep 41(3)

Song C, Lim S, Tong J(2009) Recent advances in computer-aided drug design. Brief Bioinform10(5): 579-591

Zhong F, Xing J, Li X, Liu X, Fu Z, Xiong Z, Lu D, Wu X, Zhao J, Tan X, Li F, Luo X, Li Z, Chen K, Zheng M. , Jiang H(2018) Artificial intelligence in drug design. Sci China Life Sci 61(10): 1191-1204

RESEARCH ARTICLE
Bull Biotechnol (2022) 3(2):32-38
https://doi.org/10.51539/biotech.1149287 Journal homepage: www.dergipark.org.tr/biotech

Bulletin of Biotechnology

Antiplamodial effect of sulfadoxine/pyrimethamine/clindamycin: A study in parasitized mice

Elias Adikwu[1*], Igono Simeon Ajeka[2], Confidence Ogechi Nworgu [2]

[*1]*Department of Pharmacology/Toxicology, Faculty of Pharmacy, Niger Delta University, Bayelsa State, Nigeria*
[2]*Department of Biology, Faculty of Natural and Applied Sciences, Ignatius Ajuru University of Education, Rumuolumeni, Port Harcourt, Rivers State, Nigeria*

*Corresponding author : adikwuelias@gmail.com
Orcid No: https://orcid.org/0000-0003-4349-8227

Received : 27/07/2022
Accepted : 23/12/2022

Abstract: Triple antimalarial combination therapies may overcome the emergence of antimalarial drug resistance. Sulfadoxine/pyrimethamine (S/P) is an antimalarial drug. Clindamycin (C) has potential antiplasmodial effect. This study assessed whether the antiplasmodial activity of S/P can be augmented by C on *Plasmodium berghei*-infected mice. Adult Swiss albino mice (25-30g) were grouped and infected with *Plasmodium berghei*. The mice were orally treated daily with S/P (21.4/10.7 mg/kg), C (10mg/kg) and S/P/C, respectively using curative, prophylactic and suppressive tests. The normal and negative controls were treated daily with normal saline (0.2mL) while the positive control was orally treated with chloroquine (CQ) (10mg/kg). After treatment, blood samples were collected and evaluated for percentage parasitamia and hematological parameters. Mice were observed for mean survival time. In the curative, suppressive and prophylactic tests, S/P/C significantly decreased parasitamia levels when compared to SP or C at $p< 0.05$. S/P/C significantly prolonged mean survival time when compared to S/P or C with difference at $p< 0.05$. S/P, C, and S/P/C produced 65.62 %, 62. 03 % and 85.31 % parasitamia inhibitions, respectively while CQ produced 83.72 % parasitamia inhibition. S/P/C caused significant reduction in anemia marked by increased packed cell volume, hemoglobin, red blood cells and decreased white blood cells at $p< 0.05$ when compared to SP or C. S/P/C eradicates liver merozoites and central vein congestion. C increased the antiplasmodial activity of S/P, therefore S/PC may be used for malaria treatment.

Keywords: Triple regimen, drug, combination, antimalaria, mice

1 Introduction

Plasmodium resistance, which emerged slowly after the introduction of antimalarial drug is widespread and has become a serious challenge to malaria treatment and eradication (Feachem et al., 2018; Ashley et al., 2014). *Plasmodium* resistance against sulfadoxine-pyrimethamine and chloroquine and most recently artemisinin-based combination therapies (ACTs) has been documented. This shows the need for antimalarial drug pipeline featuring compounds with novel modes of action or repurposed drugs until malaria eradication is achieved. While new compounds are been discovered, additional strategies are urgently needed to curb the persistent and rapid emergence of *Plasmodium* resistance to artemisinins and partner drugs (Mekonnen, 2015). This may involve the use of triple antimalarial combination therapies, which combine ACTs or other antimalarial drugs with partner drugs that are slowly eliminated. This may provide effective treatment and delay the emergence of *Plasmodium* resistance (Dini *et al.*, 2018; Vander Plijm *et al.*, 2020).

Sulfadoxine/Pyrimethamine (S/P) is used for malaria prophylaxis in pregnancy and malaria treatment. It is used as a partner drug with ACTs especially in Africa (WHO, 2012; 2015) to overcome *Plasmodium falciparum* resistance (Leslie *et al.*, 2017). However, there is an emergence of *Plasmodium* resistance to S/P and ACTs (Menard and Dondorp, 2017; Woodrow and White, 2017). The emergence of *Plasmodium* resistance has increased the search for novel antimalarial drugs, including partners' drugs through convectional and non-convection methods (Kremsner *et al.*, 1994).

Clindamycin (C) is a lincosamide antibiotic used for the treatment of anaerobic and gram positive bacterial infections, *Pneumocystis carinii* pneumonia, toxoplasmosis and babesiosis. C acts by inhibiting bacterial protein synthesis at the level of 50S ribosome (Smeija, 1998). Studies showed it is effective against malaria caused by *Plasmodium falciparum*, malaria. Improved effectiveness, shortened

duration of treatment and reduced risk of treatment failure were observed when it was used as a partner drug with quinine and chlroquine (Obonyo and Juma, 2012). Also, in combination with quinine it produced high malaria cure rate in mothers and children (Obonyo and Juma, 2012). This study evaluated whether C can be repurposed as a partner drug with S/P for the treatment of malaria using a mouse model infected with *Plasmodium berghei.*

2 Materials and Method

2.1 Animals, drugs and dose selection

Swiss albino mice (25–30 g) were obtained from the Animal House, of the Department of Pharmacology, Faulty of Basic Clinical Sciences, University of Port Harcourt, Nigeria. The mice were housed in plastic cages with access to chow and water *ad libitum*. The mice were acclimated for 2 weeks and handled according to the guide on animal handling by European council and the Parliament. Ethical approval for this study was provided by the Research Ethics Committee of the Department of Pharmacology/Toxicology, Faculty of Pharmacy, Niger Delta University. S/P (Artepharm Co., Ltd., China), C (Mediplantex National Pharmaceutical, Viet Nam) and CQ (Evans Pharm, Nigeria) were used. The doses used are S/P (21.4/10.7 mg/kg) (Chaponda *et al.,* 2021), C (2.2 mg/kg) (Gaillard *et al.,* 2015) and CQ (10mg/kg) (Somsak *et al.,* 2018)

2.2. Inoculation of mice with parasite

CQ sensitive *Plasmodium berghei* (NK65) was supplied in parasitized mice by the Nigerian Institute of Medical Research Yaba, Lagos. The parasite was preserved by blood passage intraperitoneally (ip) from parasitized mice to non-parasitized mice within 5–6 days of infection.

2.3. Antiplasmodial assessment of sulfadoxine/pyrimethamine/clindamycin

2.3.1. Curative test

It was performed as explained by Ryley and Peters 1980. Thirty Swiss albino mice infected i.p with 1×10^7 *Plasmodium berghei* were randomized into 6 groups of n=5/group. The normal and negative controls were treated orally with normal saline (0.2mL) while the positive control was orally treated with CQ (10mg/kg). Other groups were orally treated with S/P (21.4/10.7 mg/kg), C (2.2 mg/kg) and S/P/C, respectively. On the 5th day, tail blood samples were collected and thin blood films were prepared on slides. The slides were fixed in methanol and stained with Giemsa stain. The stained slides were viewed using a microscope and percentage parasitamia and percentage inhibitions were calculated using the formula below as reported by Adikwu and Ajeka, 2021.

$$\%\ \text{Parasitamia} = \frac{\text{Number of parasitized red blood cells (RBCs)}}{\text{Total number of RBCs count}} \times 100$$

$$\%\ \text{Inhibition} = \frac{(\%\text{Parasitamia of negative control} - \%\text{Parasitamia of treated group})}{\%\text{Parasitamia of negative control}} \times 100$$

2.3.2. Prophylactic test

It was performed based on the method described by Peters 1967. Thirty Swiss albino mice were grouped into 6 of n=5/group. The controls (normal and negative) were orally treated with normal saline (0.2mL) while the positive control was orally treated with CQ (10mg/kg) for 4 days. Other groups were orally treated with S/P (21.4/10.7 mg/kg), C (2.2 mg/kg) and S/P/C for 4 days, respectively. On the 5th day, the mice were inoculated i.p with blood containing $1x10^7$ *Plasmodium berghei*. After 72 hr tail blood samples were collected and percentage parasitamia and inhibitions were calculated as explained above.

2.3.3. Suppressive test

It was performed as reported by Knight and Peters 1980. Thirty mice inoculated i.p with blood containing $1x10^7$ *Plasmodium berghei* were grouped into 6 of n=5/group. After 2 hr, the mice were orally treated with S/P (21.4/10.7 mg/kg), C (2.2 mg/kg) and S/P/C daily for 4 days, respectively. Normal and negative controls were orally treated with normal saline (0.2mL) while positive control was treated with CQ (10mg/kg) orally for 4 days. On the 5th day, tail blood samples were collected, prepared and percentage parasitamia and inhibitions were calculated as explained above.

2.4. Evaluation of biochemical markers

Samples of blood collected from the group used for the curative test were evaluated for hemoglobin (Hb), white blood cells (WBCs), red blood cells (RBCs) and packed cell volume (PCV) with the aid of an auto analyzer.

2.5. Evaluation of mean survival time

The mice were observed for mortality and the mean survival time (MST) was calculated using the formula below reported by Adikwu and Ajeka, 2021.

$$\text{MST} = \frac{\text{Sum of survival time of all mice in a group (days)}}{\text{Total number of mice in that group}}$$

2.6. Statistical analysis

Values as mean ± SEM (standard error of mean) of n=5. One-way analysis of variance (ANOVA) and Tukey's *post hoc test* were used for data analysis. Significance was set at $p< 0.05$.

3. Results

3.1.Curative effect of sulfadoxine/ pyrimethamine/ clindamycin on mice infected with *Plasmodium berghei.*

Treatment with S/P/C decreased percentage parasitamia with significant difference observed at $p<0.05$ when compared to treatment with S/P or C. S/P, C and S/P/C showed 65,62%, 62.03% and 85.31% inhibitions, respectively whereas CQ produced 83.27% inhibition (Table 1). Treatment with S/P/C significantly prolonged MST with difference observed at $p<0.05$ when compared to treatment with S/P or C (Table.1).

3.2. Prophylactic effect of sulfadoxine/ pyrimethamine/ clindamycin on mice infected with *Plasmodium berghei*

Treatment with S/P/C decreased percentage parasitamia with significant difference observed at $p<0.05$ when compared to treatment with S/P or C (Table 2). The inhibitions which represent 75.22%, 72.27%, 97.76% and 96.25 % were produced by S/P, C, S/P/C and CQ, respectively (Table.2). S/P/C prolonged MST significantly with difference observed at $p<0.05$ when compared to S/P or C (Table 2).

3.3. Suppressive effect of sulfadoxine/ pyrimethamine/ clindamycin on mice infected with *Plasmodium berghei*

S/P/C decreased percentage parasitamia significantly when compared to S/P or C with difference observed at $p<0.05$. The inhibitions produced by S/P, C and S/P/C represent 72.40%, 70.63% and 94.38%, respectively while CQ produced 93.80% inhibition (Table 3). S/P/C prolonged MST with significant difference observed at $p<0.05$ when compared to S/P or C (Table 3).

3.4. Effect of sulfadoxine/pyrimethamine/clindamycin on hematological indices of mice infected with *Plasmodium berghei*

Reduced RBCs, PCV and Hb and increased WBCs occurred significantly ($p<0.05$) in *Plasmodium bergei* infected mice (Table 4). However, treatment with S/P/C significantly increased RBCs, PCV, Hb and significantly decreased WBCs with difference observed at $p<0.05$ when compared to S/P or C (Table 4).

3.5. Effect of sulfadoxine/pyrimethamine/clindamycin on liver histology of mice infected with *Plasmodium berghei*

The liver of normal control mice showed normal histology (Figure 6a) whereas the liver of the negative control showed normal hepatocytes, congested sinusoids, central vein congestion and merozoites (Figures 6b and 6c). The liver of CQ-treated mice showed normal hepatocytes and central vein congestion (Figure 6d). The liver of C-treated mice showed central vein congestion, and merozoites (Figure 6e) while the liver of S/P treated mice (Figure 6f) and the liver of S/P/C-treated mice (Figure 6g) showed normal hepatocytes and congested Sinusoids.

Table 1. Curative effect of sulfadoxine/pyrimethamine/clindamycin on mice infected with *Plasmodium berghei.*

Treatment	% Parasitamia	% Inhibition	MST (Days)
NC	31.26±1.23	0.0	9.05±0.97
CQ	5.09±0.11[a]	83.72	27.6±3.10 [a]
S/P	10.75±0.15[b]	65.62	22.1±3.22 [b]
C	11.86±0.88[b]	62.03	20.4±2.12 [b]
S/P/C	4.59±0.02[a]	85.31	30.8±4.07 [c]

Data as mean± standard error of mean, n=5, NC: Negative control, CQ: Chloroquine (Positive control), C: Clindamycin, S/P: Sulfadoxine/pyrimethamine, MST: Mean survival time. Values with difference superscripts down the column significantly differ at $p<0.05$ (ANOVA)

Table 2. Prophylactic effect of sulfadoxine/pyrimethamine/clindamycin on mice infected with *Plasmodium berghei*

Treatment	% Parasitamia	% Inhibition	MST (Days)
NC	22.25±0.68	0.0	9.61±0.16
CQ	0.83±0.20 [a]	96.25	34.15±3.01[a]
S/P	5.51±0.01 [b]	75.22	29.86±3.40[b]
C	6.17±0.77 [b]	72.27	27.54±3.21[b]
S/P/C	0.50±0.01 [a]	97.76	37.71±5.10[a]

Data as mean± standard error of mean, n=5, NC: Negative control, CQ: Chloroquine (Positive control), C: Clindamycin, S/P: Sulfadoxine/pyrimethamine. MST: Mean survival time. Values with difference superscripts down the column significantly differ at $p<0.05$ (ANOVA: Analysis of variance)

Table 3. Suppressive effect of sulfadoxine/pyrimethamine/clindamycin on mice infected with *Plasmodium berghei*

Treatment	% Parasitamia	% Inhibition	MST (Days)
NC	27.86±2.10	0.00	9.23±0.13
CQ	1.72±0.20 [a]	93.80	30.26±3.17[a]
S/P	7.69±0.16 [b]	72.40	28.73±3.25[b]
C	8.18±0.53 [b]	70.63	25.14±3.44[b]
S/P/C	1.58±0.04 [a]	94.38	33.08±7.03[a]

Data as mean± standard error of mean, n=5, Negative control, CQ: Chloroquine (Positive control), C: Clindamycin, S/P: Sulfadoxine/pyrimethamine. MST: Mean survival time. Values with difference superscripts down the column significantly differ at $p<0.05$ (ANOVA: Analysis of variance)

Table 4. Effect of sulfadoxine/pyrimethamine/clindamycin on hematological indices of mice infected with *Plasmodium berghei*

Treatment	RBCs ($x10^6$)	WBCs (cells/L)	PCV (%)	Hb (g/dL)
NM	6.85±0.02	4.76±0.40	58.54±5.18	15.64±0.38
NC	2.00±0.46 [b]	12.94±0.11[b]	20.56±3.10 [b]	6.36±0.26 [b]
CQ	5.67±0.73 [c]	5.35±0.30 [c]	49.61±6.35[c]	14.27±0.41[c]
S/P	3.35±0.15 [d]	8.77±0.36 [d]	34.74±4.98[d]	10.50±0.47[d]
C	3.10±0.27 [d]	9.63±0.52 [d]	31.17±3.55 [d]	10.01±0.31[d]
S/P/C	5.94±0.56 [c]	5.00±0.30 [c]	52.03±5.13 [c]	14.95±1.33[c]

Data as mean± standard error of mean, n=5, NM: Normal control, NC: Negative control, CQ: Chloroquine (Positive control), C: Clindamycin, S/P: Sulfadoxine/pyrimethamine. RBCs: Red blood cells, WBCs: White blood cells, PCV: Packed cell volume, Hb: Hemoglobin, Values with difference superscripts down the column significantly differ at $p<0.05$ (ANOVA: Analysis of variance)

4. Discusion

Malaria is a public health problem that affects mostly people living in Sub-Sahara Africa. Children below age 5 are the most vulnerable group affected, with an estimate of 67% (247,000) of all malaria mortality worldwide (Ashley *et al.,* 2004). The increasing prevalence of drug resistant parasites now threatens the efficacies of antimalarial drugs in Sub-Saharan African (Targett *et al.,* 2001). There is currently a concerted effort to evaluate new antimalarial drug combinations through drug repurposing. The discovery of new antimalarial drug combinations can reduce post treatment parasite transmission so as to counteract the transmission of drug resistant parasites (Mekommen. 2015). The present study aim at assessing whether C can augment the antimalarial activity of S/P in a mouse model infected with *Plasmodium berghei*. A 4 day curative test was used to evaluate the antiplasmodial activity of the drug combination on establishment infection whereas suppressive test was used to determine the antiplasmodial activity on early infection (Fidock *et al.,* 2014). Mouse model was used for this study, because it allows the investigation of long term immunity to *Plasmodium* parasites, disease progress and permits studies of organs to which the parasite sequesters, such as the spleen and liver which is difficult in humans (Wykes, 2009). Many of the antimalarial drugs used currently emerged from small molecules, whose antimalarial activities were assessed in animal models (Peter *et al.,* 1998). *Plasmodium berghei* was used for this study, because of its ability to sequester within the micro-circulation, which is the characteristic of severe malaria especially the cerebral form. [7] In this study, S/P/C decreased percentage parasitamia in the curative and suppressive tests with similar effect as the standard (CQ). Also, in the prophylactic test, S/PC decreased percentage parasitamia with similar effect as CQ. In addition to the antiplasmodial assessment of S/P/C, the current study further assessed its impact on MST. In the curative, prophylactic and suppressive tests, S/P/C prolonged MST most than its constituent drugs. Also, the prolongation of MST by S/P/C was at par with CQ. Anemia, a common complication of malaria is a consequence of the hemolysis of infected and uninfected erythrocytes and bone marrow dyserythropoiesis by *Plasmodium* parasites (White, 2018). This study observed anemic signs in *Plasmodium berghei* infected mice characterized by altered levels of hematologic indices which support earlier reports (Georgewwill *et al.,* 2021). However, treatment with S/P/C curtailed the anemic impact of *Plasmodium berghei*. The colonization of the liver by *Plasmodium* parasites is an integral part of malaria infection. After an infectious mosquito bite, sporozoites find their way to hepatocytes, where liver stage development occurs. A single infectious mosquito bite can lead to liver infection, which sets the stage for successful host colonization by *Plasmodium* parasites (Vaughan and Kappe, 2017).

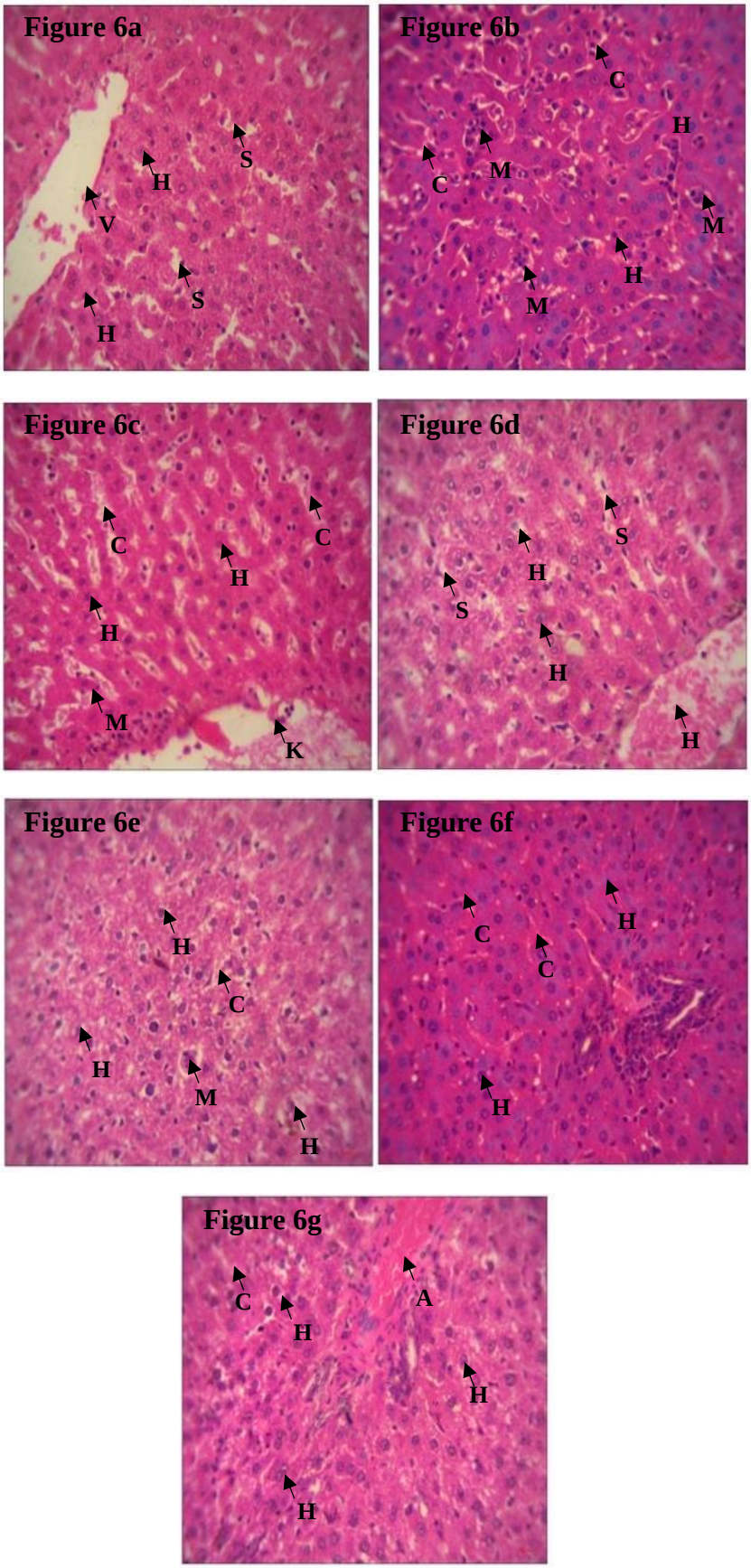

Figures 6a-6g. Liver micrographs of the control and experimental mice. Figure 6a: control mice, Figures 6b and 6c: Parasitized mice. Figure 6d: Treatment with chloroquine. Figure 6e: Treatment with clindamycin. Figure 6f: Treatment with sulfadoxine/pyrimethamine. Figure 6g: Treatment with sulfadoxine/pyrimethamine/clindamycin. V: Central vein K: Central vein congestion, M: Merozoites, S: Sinusoids, C: Congested sinusoids, H: Normal hepatocytes. A: Hepatic artery. X 400 H&E

This makes it imperative for the assessment of the antiplasmodial effect of drug candidates at the liver stage of infection. In this study, congested sinusoid, merozoites and central vein congestion were observed in the liver of *Plasmodium berghei*-infected mice, which support earlier reports (Ooji, 2009; Udonkang et al., 2018). The aforementioned liver changes were eradicated in mice treated with S/P/C. This observation showed that S/P/C may cure the liver stage of *Plasmodium* infection. The observed antiplasmodial activity of S/P/C may be due to the abilities of its constituent drugs to target *Plasmodium* parasites at different sites. S/P inhibits dihydrofolate reductace and dihydropteorate synthase in *Plasmodium* parasites thereby preventing folic acid synthesis (Hayton *et al.*, 2002). C inhibits protein synthesis in bacteria via activity at 50s ribosome, but its antiplasmodial activity is attributed to the inhibition of *Plasmodium* apicoplast (Lell and Kremsner, 2002; Goodman et al., 2013).

5. Conclusion: The present study showed that C increased the antiplasmodial activity of S/PC by inhibiting blood and liver stages of *Plasmodium berghei* infection. This study suggests the use of S/P/C for the treatment of malaria.

Authors contributions. EA: study conception, design, supervision, sample collection, and data analysis, literature review and manuscript writing and editing. ISA: Design, supervision, animal handling, data analysis, literature review and manuscript writing. CON: Design, supervision, animal handling, data analysis, literature review and manuscript writing.

Conflict of interest: The authors declare no conflict of interest

Source of financial: None.

References

Adikwu E, Ajeka IS (2021). Artemether/ lumefantrine/ clindamycin eradicates blood and liver stages of Plasmodium berghei infection in mice J Anal Pharm Res. 10(6):240–244

Ashley EA, Dhorda M, Fairhurst RM, Amaratunga C, Lim P, Suon S et al. (2014). Spread of artemisinin resistance in Plasmodium falciparum malaria. N Engl J Med. 371: 411–23.

Chaponda EB, Mharakurwa S, Michelo C, Bruce J, Chandramoha D, Chico M et al. (2021). Sulfadoxine-pyrimethamine parasitological efficacy against Plasmodium falciparum among pregnant women and molecular markers of resistance in Zambia: an observational cohort study. Malar J. 20(1):61.

Dini S, Zaloumis S, Cao P, Price RN, Fowkes FJI, van der Pluijm RW et al. (2018). Investigating the Efficacy of Triple Artemisinin-Based Combination Therapies for Treating Plasmodium falciparum Malaria Patients Using Mathematical Modeling. Antimicrob Agents Chemother. 24;62(11):e01068-18

Feachem RGA Chen I, Akbari O, Bertozzi-villa M, Bhatt S, Binka F et al. (2019). Malaria eradication within a generation: ambitious, achievable, and necessary. *Lancet.* 394: 1056-1112

Fidock DA, Rosenthal PJ, Croft SL, Brun R, Nwaka S (2004). Antimalarial drug discovery: efficacy models for compound screening. Nat Rev Drug Discov. 3: 509-520

Gaillard T, Madamet M, Pradines B. (2015) Tetracyclines in malaria. Malaria J. 14(445):1-10.

Georgewill UO, Nwakaego OE, Adikwu (2021). Antiplasmodial activity of desloratadine-dihydroartemisinin-piperaquine on *Plasmodium berghei* in infected mice. J App Biol Biotech. 9(2): 169-173.

Goodman CD, Useglio M, Peirú S, Labadie GR, McFadden GI, Rodríguez E, et al. (2013). Chemobiosynthesis of new antimalarial macrolides. Antimicrob Agents Chemother. 57:907–13.

Hayton K, Ranford-Cartwright LC , Walliker D. (2002). Sulfadoxine-Pyrimethamine Resistance in the Rodent Malaria Parasite *Plasmodium chabaud.* Antimicrob Agents and Chem. 46 (8): 2482-2489.

Knight DJ, PetersW. (1980). The antimalarial action of N-Benzyl oxydihydrotriazines and the studies on its mode of action. Ann of Trop Med Parasitol. 74: 393-404.

Kremsner PG, Winkler S, Brandts C, Neifer S, Bienzle U, Graninger W: (1994). Clindamycin in combination with chloroquine or quinine is effective therapy for uncomplicated falciparum malaria in children from Gabon. J Infect Dis.169:467-470.

Lell B, Kremsner PG (2002). Clindamycin as an Antimalarial Drug: Review of Clinical Trials Antimicrobial agents and chemotherapy. 46 (8) 2315–2320.

Leslie T, Mayan MI, Hassan MA, Safi MH, Klinkenberg E, Whitty CJ (2007). Sulfadoxine-pyrimethamine, Chloroproguanil-Dapsone, or Chlorquine for the treatment of Plasmodium Vivax malaria in Afghanistan and Pakistan: A randomized controlled trial, JAMA. 297(20): 2201.

Mekonnen LB. (2015). In vivo antimalarial activity of the crude root and fruit extracts of Croton macrostachyus (Euphorbiaceae) against Plasmodium berghei in mice. J Tradit Complement Med. 4;5(3):168-73

MenardD and Dondorp A. (2017). Antimalarial Drug Resistance: A Threat to Malaria Elimination. Cold Spring Harb. Perspect. Med. (7) 7: 025619.

Obonyo CO and Juma EA. (2012). Clindamycin plus quinine for treating uncomplicated falciparum malaria: a systematic review and meta-analysis. Malar J. 11: 2.

Ooji CV. (2009). The fatty liver stage of malaria parasite. Nature reviews micro biology. (2): 94-95.

Peter I.T., Anatoli V.K. ASM Press; Washington, DC: 1998. The Current Global Malaria Situation. Malaria Parasite Biology, Pathogenesis, and Protection; pp. 11–22

PetersW. (1967). Rational methods in the search for antimalarial drugs. Transaction of Royal. Soc Trop Med Hyg. 3; 400-410

RyleyJF PetersW. (1970). The antimalarial activity of some quinolone esters. Annals of Tropical Medicine and Parasitology.84: 209-222.

Smieja M. (1998). Current indications for the use of clindamycin: A critical review. Can J Infect Dis. 9(1):22-8.

Somsak V, Damkaew A, Onrak P. (2018). Antimalarial activity of kaempferol and its combination with chloroquine in *Plasmodium berghei* infection in mice. JPathol. 2018; 1-7.

Targett G, Drakeley C, Jawara M, VonSeidlein L, Coleman R, Deen J et al. (2001). Artesunate reduces but does not prevent post treatment transmission of *Plasmodium falciparum* to Anopheles gambiae, J Infect Dis.2001; 183: 1254-1259.

Udonkang MA, Eluwa BK, Enun, PC, Inyang-EtohIJ. Inyang I. (2018). Studies on antimalarial activity and liver histopathological changes of artocarpus altilis on plasmodium berghei-infected mice. RJLBPCS 4(3): 106-114.

van der Pluijm RW, Tripura R, Hoglund RM, Phyo AP, Lek D, Islam A et al., (2020). Triple artemisinin-based combination therapies versus artemisinin-based combination therapies for uncomplicated Plasmodium falciparum malaria: a

multicentre, open-label, randomised clinical trial Lancet. 395: 1345–60

Vaughan AM and Kappe SH. (2017). Malaria Parasite Liver Infection and Exoerythrocytic Biology. Cold Spring Harb Perspect Med. 7(6): 025486, 1-21.

White, N.J. Anaemia and malaria (2018). Malar J. 17(371): 1-17.

WoodrowCJ, White NJ. (2017). The clinical impact of artemisinin resistance in Southeast Asia and the potential for future spread. FEMS Microbiol. Rev. 41: 34–48.

World Health Organization (WHO). The selection and use of essential medicines. Twentieth report of the WHO, expert committee. (including 19th WHO model list of essential medicines for children). WHO technical report seriesGeneva. World Health Organization.2015; 994.

World Health Organization (WHO). Updated WHO policy recommendation: intermittent preventive treatment of malaria in pregnancy using sulfadoxine-pyrimethamine (IPTp-SP). Geneva, World Health Organization; 2012.

Wykes MN, Good MF. (2009).What have we learnt from mouse models for the study of malaria? 39(8): 2004-2007.

RESEARCH ARTICLE
Bull Biotechnol (2022) 3(2):39-44
https://doi.org/10.51539/biotech.1178308 Journal homepage: www.dergipark.org.tr/biotech

Bulletin of Biotechnology

In Silico Approach For Detection Of The Effect Of *UGT1A1* Polymorphisms On Telmisartan Response

Gizem Koprululu Kucuk*

*[1]*Department of Radiotherapy, Istanbul Sisli Vocational School, Istanbul, Turkey*

*Corresponding author: gzm0507@gmail.com
Orcid No: https://orcid.org/ 0000-0001-6667-4532

Received : 21/09/2022
Accepted : 23/12/2022

Abstract: Hypertension is a cardiovascular disease that manifests itself with a continuous increase in systemic arterial blood pressure and can lead to serious complications over time. It is estimated that 37% of hypertensive patients receive treatment and one-third of them are under control. Telmisartan is an angiotensin receptor blocker used in the treatment of hypertension. Uridine 5'-diphospho-glucuronyltransferase 1 (UGT1A1) gene encodes the Uridine 5'-diphospho-glucuronyltransferase (UGT) enzyme and metabolizes the telmisartan. Single nucleotide polymorphisms cause amino acid, protein structure, and function to change. These changes affect the drug response and therapy. Polymorphisms of the UGT1A1 gene (rs4148323, rs28934877) cause telmisartan resistance. In this study, the SWISS-MODEL database and Chimera 1.15 ver. Programs were used to create homology models. The HOPE database was used to calculate the damage of mutation on protein structure and show the mutation effects on protein. The HDock server was used to demonstrate interactions between telmisartan and wild-type protein and, mutant type protein. It was detected that the mutant residue of *UGT1A1* (rs4148323) is located in an important domain for protein activity. Mutation might disturb the protein function. rs28934877 is likely damaging to the protein. These mutations cause the loss of interactions and affect the drug response. By docking analysis, Telmisartan drug interactions were shown between wild and mutant types protein Possible drug conformation is designed for the effective treatment of patients carrying the common mutation.

Keywords: Telmisartan; docking; Single nucleotide polymorphism (SNP); hypertension; *UGT1A1; in silico*

1 Introduction

Hypertension is the third leading cause of death in the world and causes 12,8% of adult deaths (https://www.who.int/gho/ncd/risk_factors/blood_pressure_prevalence_text/en). It is estimated that 9,4 million individuals die because of hypertension and complication related to hypertension (http://www.who.int/). It has been shown by the World Health Organization data that 45% of deaths due to heart diseases and 51% due to stroke in developing countries are caused by hypertension (Kılıc et al. 2016). Moreover WHO predicts that the prevalence of hypertension will reach 29,2%, and the number of patients with hypertension will be 1.56 billion worldwide in 2025 (WHO 2015 http://www.who.int/ Accessed: 14.08.2022).

Hypertension is defined as the high pressure exerted by the blood in the blood vessels against the vessel wall. If this high blood pressure continues for a long time, this causes damage to the vessel. If a person measures diastolic blood pressure higher than 90 mmHg and systolic blood pressure higher than 140 mmHg in three different measurements, this will be enough to define hypertension (Martinez-Quinones et al. 2018).

Many risk factors may cause the development of hypertension in a person. The risk of hypertension increases with advancing age (Huang et al. 2018). Family stories may also affect the development of hypertension risk. Being overweight, do not perform physical activity, or smoking tobacco are also considered risk factors for the development of hypertension (Papathanasiou et al. 2015). Molecular genetic studies show that hypertension is an inherited disease. Genetic and environmental factors are responsible for the development of hypertension (Ding et al. 2018).

There are pharmacological and nonpharmacological approaches to hypertension therapy. Telmisartan is a pharmacological approach for the hypertension therapy. It is a nonpeptide molecule. Its molecular weight is 514.63. It has a pH between three and nine and is soluble in strong bases (Sweetman, 2007). Telmisartan is an angiotensin receptor

blocker used in the treatment of hypertension (Sharpe et al. 2001). It is well absorbed in the gastrointestinal tract. It is highly bound to plasma proteins. Telmisartan competes with angiotensin and antagonizes the binding of angiotensin to the receptor and thus its effects in the therapeutic concentration range. It has a longer-lasting effect because it more effectively suppresses Angiotensin-2, which is present in the blood and increases blood pressure in the body (Sweetman, 2007). Telmisartan relaxes blood vessels. Telmisartan has been used in the treatment of hypertension since the early 2000s.

Uridine 5'-diphospho-glucuronyltransferase (UDP-5'-diphospho glucuronyltransferase, UGT) is a phase II drug metabolizing enzyme. It catalyzes the glucuronidation of compounds ,and it transfers glucuronic acid from UDP-glucuronic acid to substrates (Dutton, 1980). The uridine 5'-diphospho-glucuronyltransferase 1 (*UGT1A1*) gene encodes the UGT enzyme. The *UGT1A1* gene contains 5 exons and is located on 2q37 (Ritter et al. 1992). The *UGT1A1* gene encodes the UGT enzyme and performs a chemical reaction called glucuronidation, preventing the accumulation of toxic waste in our bodies. Some genetic variations in *UGT1A1* reduce the enzymatic activity of UGT, which impairs the body's ability to detox and causes toxic substances to accumulate in the body. *UGT1A1* is one of the primary genetic variants responsible for reduced detox ability. UGT enzyme metabolizes the telmisartan in the body (Yamada et al. 2011). Glucuronidation of telmisartan was shown in Figure 1.

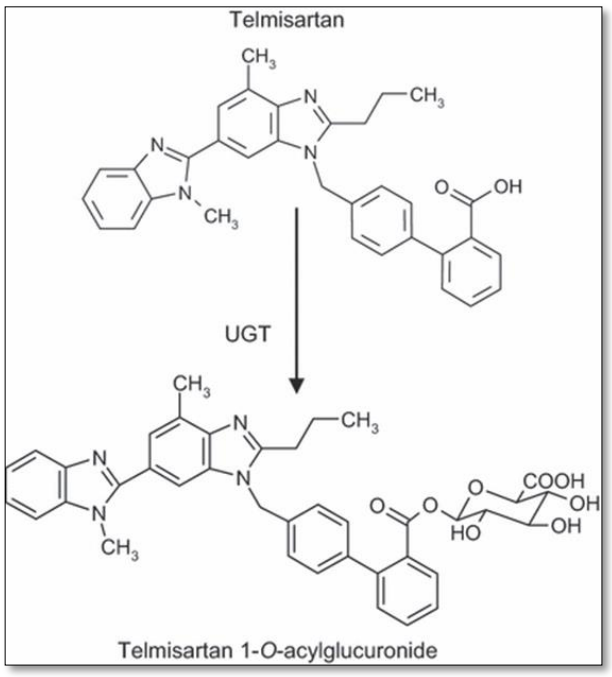

Fig 1. Glucuronidation of telmisartan (Ebner et al. 2012).

Lu Huang et al. found that genetic polymorphisms of *UGT1A1* (rs4148323) were effective on blood pressure and plasma telmisartan concentration in patients with hypertension (Huang et al. 2019). In the studies, it was determined that the rs28934877, rs34993780 mutation in the UGT1A1 gene plays an effective role in the development of hypertension, heart failure, and cardiac disorders, and increases the risk of developing heart failure and hypertension (Di et al. 2009; Zhang et al. 2012; Maruo et al. 2000). Studies on the subject show that mutations in the *UGT1A1* gene play a role in the development of hypertension (Bosma et al. 2003; Schewertner et al. 2008).

2 Materials and Method

2.1 Homology Modeling Databases

The Genebank database of the National Center for Biotechnology Information, USA, NCBI was used to detect pathogenic SNPs of the *UGT1A1* gene (https://www.ncbi.nlm.nih.gov/ Access date: 20.08.2022). Two SNPs (rs4148323, rs28934877) were selected to relate hypertension and Telmisartan response on the database. Genebank database of the National Center for Biotechnology Information, USA, NCBI serves the FASTA format of an amino acid sequence of the UGT1A1 gene (https://www.ncbi.nlm.nih.gov/ Access date: 20.08.2022). The amino acid sequence of wild type and mutant types were shown in Table 1.

Table 1. The amino acid sequence of wild-type and mutant types (https://www.ncbi.nlm.nih.gov/ Access date: 20.08.2022).

UGT1A1

MAVESQGGRPLVLGLLLCVLGPVVSHAGKILLIPVDG
SHWLSMLGAIQQLQQRGHEIVVLAPDASLYIRDGAFY
TLKTYPVPFQREDVKESFVSLGHNVFENDSFLQRVIK
TYKKIKKDSAMLLSGCSHLLHNKELMASLAESSFDV
MLTDPFLPCSPIVAQYLSLPTVFFLHALPCSLEFEATQ
CPNPFSYVPRPLSSHSDHMTFLQRVKNMLIAFSQNFL
CDVVYSPYATLASEFLQREVTVQDLLSSASVWLFRSD
FVKDYPRPIMPNMVFVGGINCLHQNPLSQEFEAYINA
SGEHGIVVFSLGSMVSEIPEKKAMAIADALGKIPQTVL
WRYTGTRPSNLANNTILVKWLPQNDLLGHPMTRAFIT
HAGSHGVYESICNGVPMVMMPLFGDQMDNAKRMET
KGAGVTLNVLEMTSEDLENALKAVINDKSYKENIMR
LSSLHKDRPVEPLDLAVFWVEFVMRHKGAPHLRPAA
HDLTWYQYHSLDVIGFLLAVVLTVAFITFKCCAYGYR
KCLGKKGRVKKAHKSKTH

rs4148323

MAVESQGGRPLVLGLLLCVLGPVVSHAGKILLIPVDG
SHWLSMLGAIQQLQQRGHEIVVLAPDASLYIRD**R**AFY
TLKTYPVPFQREDVKESFVSLGHNVFENDSFLQRVIK
TYKKIKKDSAMLLSGCSHLLHNKELMASLAESSFDV
MLTDPFLPCSPIVAQYLSLPTVFFLHALPCSLEFEATQ
CPNPFSYVPRPLSSHSDHMTFLQRVKNMLIAFSQNFL
CDVVYSPYATLASEFLQREVTVQDLLSSASVWLFRSD
FVKDYPRPIMPNMVFVGGINCLHQNPLSQEFEAYINA
SGEHGIVVFSLGSMVSEIPEKKAMAIADALGKIPQTVL
WRYTGTRPSNLANNTILVKWLPQNDLLGHPMTRAFIT
HAGSHGVYESICNGVPMVMMPLFGDQMDNAKRMET
KGAGVTLNVLEMTSEDLENALKAVINDKSYKENIMR
LSSLHKDRPVEPLDLAVFWVEFVMRHKGAPHLRPAA
HDLTWYQYHSLDVIGFLLAVVLTVAFITFKCCAYGYR

KCLGKKGRVKKAHKSKTH

rs28934877

MAVESQGGRPLVLGLLLCVLGPVVSHAGKILLIPVDG
SHWLSMLGAIQQLQQRGHEIVVLAPDASLYIRDGAFY
TLKTYPVPFQREDVKESFVSLGHNVFENDSFLQRVIK
TYKKIKKDSAMLLSGCSHLLHNKELMASLAESSFDV
MLTDPFLPCSPIVAQYLSLPTVFFLHALPCSLEFEATQ
CPNPFSYVPRPLSSHSDHMTFLQRVKNMLIAFSQNFL
CDVVYSPYATLASEFLQREVTVQDLLSSASVWLFRSD
FVKDYPRPIMPNMVFVGGINCLHQNPLSQEFEAYINA
SGEHGIVVFSLGSMVSEIPEKKAMAIADALGKIPQTVL
WRYTGTRPSNLANNTILVKWLPQNDLLGHPMTRAFIT
HAGSHGVYESICNGVPMVMMPLFGDQMDDAKRMET
KGAGVTLNVLEMTSEDLENALKAVINDKSYKENIMR
LSSLHKDRPVEPLDLAVFWVEFVMRHKGAPHLRPAA
HDLTWYQYHSLDVIGFLLAVVLTVAFITFKCCAYGYR
KCLGKKGRVKKAHKSKTH

SWISS-MODEL was used to create homology modeling of *UGT1A1* (wild type, rs4148323, and rs28934877) (Waterhouse et al. 2018). Three-dimensional models were examined with the UCSF Chimera program, which is a visualization tool (Pettersen et al. 2004). The UCSF Chimera program was used to visualize the wild and mutant (rs4148323, and rs28934877) protein structures.

2.2. Bioinformatic Analysis Of Homology Models

HOPE was used for the detection of the structural effect of the mutation. HOPE shows the mutation effects, and calculates the probable damage of mutation on the protein structure. In this study, it was shown that UGT1A1 mutation affects protein structure by the HOPE database (Venselaar et al. 2010).

2.3. Molecular Docking Study

The docking method predicts the interactions between the conformation and orientation of the ligand structure and a target binding site. Docking studies are the most important methods for drug discovery. In drug resistance studies, docking has an important role to understand the interactions between drugs and the target region. As a result, new therapies can be developed by the docking method for drug resistance in patients. Three-dimensional (3D) structures are obtained for docking studies. Docking programs are used to obtain these 3D structures. In drug discovery studies, the HDock server is usually used (Yan et al. 2017). HDock uses a genetic algorithm. Genetic algorithms transfer the energy and geometry information of a newly formed conformation of the molecule to the next conformation and thus they are obtained optimal conformations. In this study, the HDock server was used for the molecular docking study of *UGT1A1* and telmisartan. (Yan et al. 2017).

3 Results

The amino acid sequence format which is used as a basis in bioinformatics studies was created based on the NCBI-P33261 accession number sequence.

SWISS-MODEL was used to obtain three-dimensional (3D) structures and homology modeling was performed by the Swiss-Model database and the Chimera program. UGT1A1 wild and rs4148323 and rs28934877 overlapping structures were shown in Figure 1 and Figure 2.

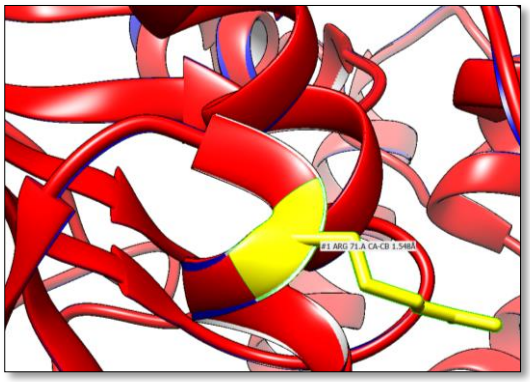

Fig 1. The ribbon structure of UGT1A1 wild-type and rs4148323 overlapping (Pettersen et al., 2004).

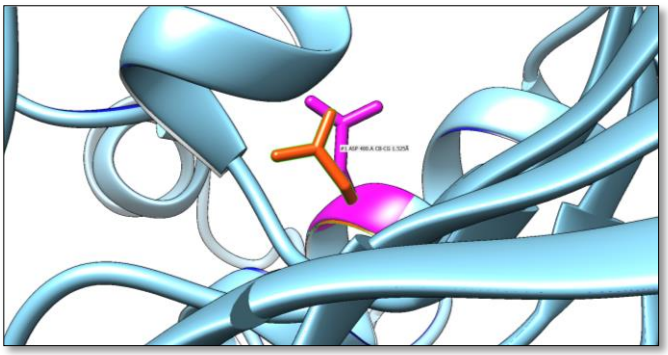

Fig 2. The ribbon structure of UGT1A1 wild-type and rs28934877 overlapping (orange is the wild type and purple is the mutant type amino acid) (Pettersen et al., 2004).

Schematic structures of the wild (left) and the mutant (right) amino acids for rs4148323 were shown in Figure 3.

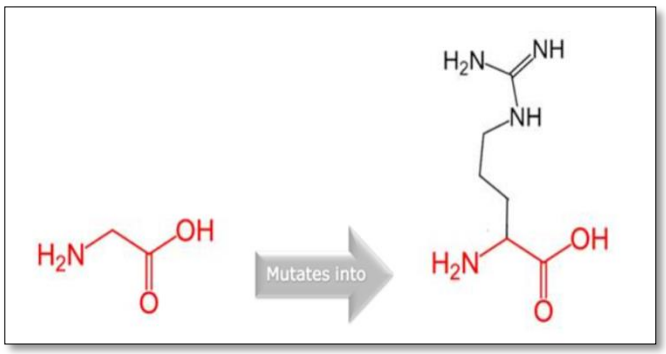

Fig 3. Schematic structures of the wild (left) and the mutant (right) amino acid (rs4148323) (Venselaar et al., 2010).

The wild-type residue is glycine and changes to Arginine at position 71 in the mutant type (rs4148323). While the wild-type residue charge had a NEUTRAL charge, the mutant residue charge was POSITIVE. It was detected that the wild-type residue was more hydrophobic than the mutant residue. Glycine is a wild-type residue and the most flexible residue. Flexibility plays an important role in protein function. Mutation of this glycine can abolish this function. These

results showed that the mutation is deleterious. The mutated residue is located in an important region for the protein's

main activity. Mutated residue might disturb the protein's main function (BMC Bioinformatics, 2010)

Schematic structures of the wild (left) and the mutant (right) amino acids for rs28934877 were shown in Figure 4.

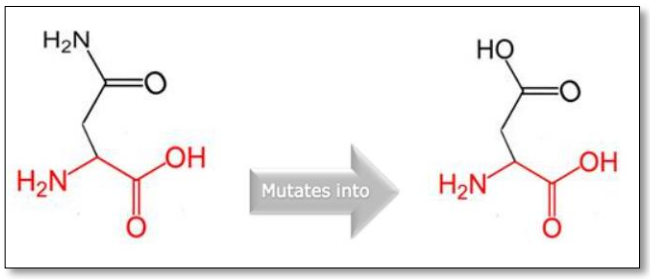

Fig 4. Schematic structures of the wild (left) and the mutant (right) amino acid (rs28934877) (Venselaar et al., 2010).

In rs28934877, the Asparagine amino acid was changed to an Aspartic acid at position 400. While the wild-type residue had a NEUTRAL charge, the mutant residue charge was NEGATIVE. It was detected that this mutation is probably damaging to the protein.

Amino acid changing was demonstrated in Figures 5 and 6 for rs4148323 and rs28934877.

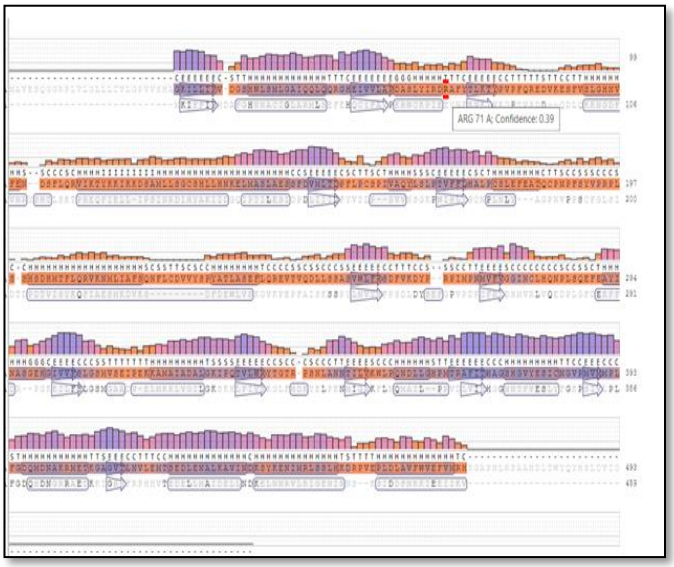

Fig 5. rs4148323 amino acid sequence and amino acid change (Pettersen et al. 2004)

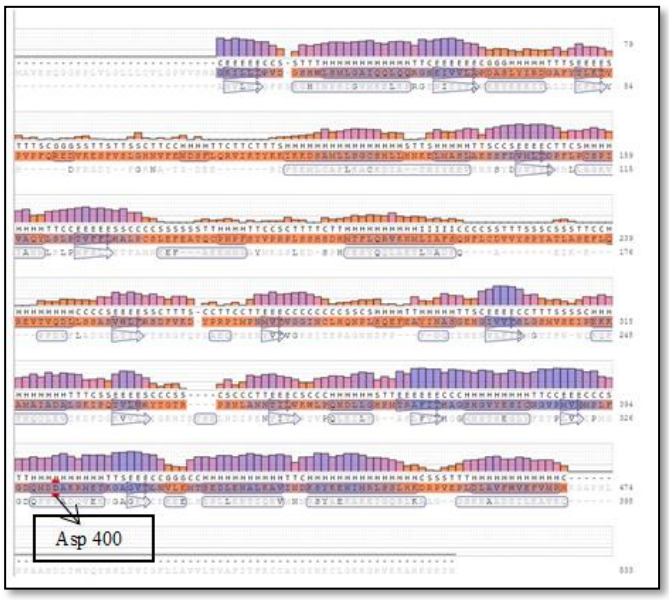

Fig 6. rs28934877 amino acid sequence and amino acid change (Pettersen et al. 2004)

HDock server and BIOVA Discovery Studio were used for the molecular docking study between telmisartan and UGT1A1. HDock and BIOVA Discovery Studio is used Bioinformatics-based methods to predict the structure and generate interactions (Yan Y. et al., 2017; https://3ds.com/productsservices/biovia/products).
Telmisartan docking results were shown in Figure 7-9.

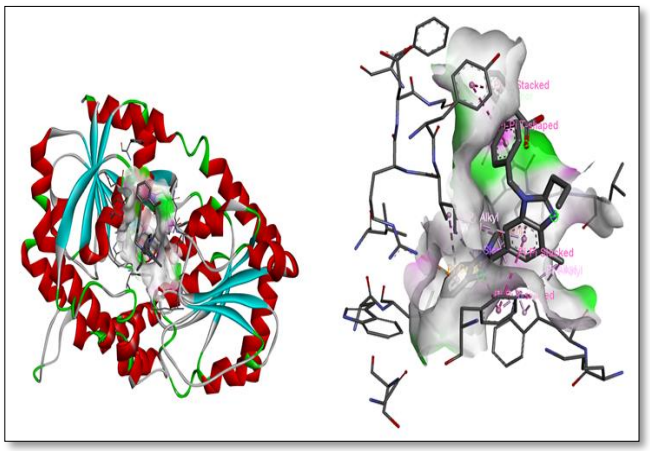

Fig 7. Visualization of the UGT1A1 (wild) complex and telmisartan docking via BIOVIA Discovery Studio (https://3ds.com/productsservices/biovia/products).

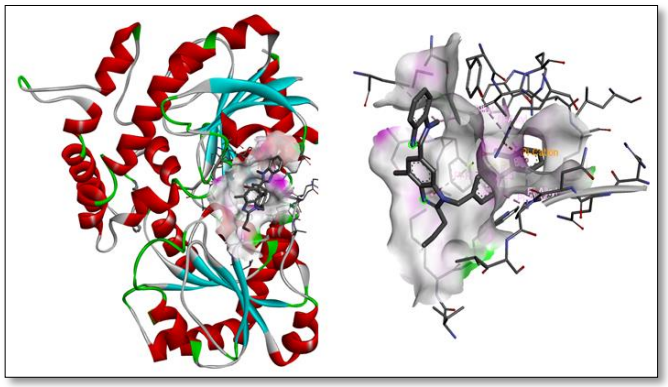

Fig 8. Visualization of the rs4148323 complex and telmisartan docking via BIOVIA Discovery Studio (https://3ds.com/productsservices/biovia/products).

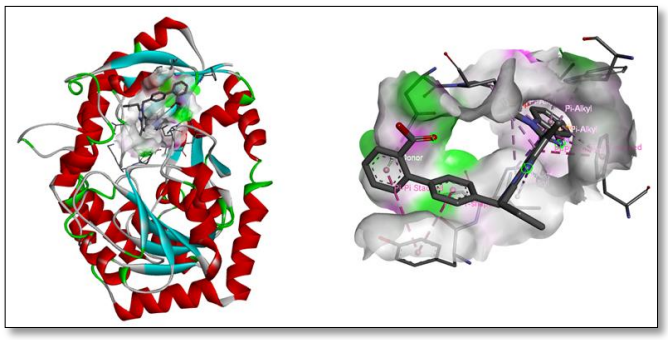

Fig 9. Visualization of the rs28934877 complex and telmisartan docking via BIOVIA Discovery Studio (https://3ds.com/productsservices/biovia/products).

4 Discussion

Telmisartan is a blocker of angiotensin II receptor . It is widely used in the treatment of hypertension in the clinic. Telmisartan is metabolised by UGTs (Shin HJ. et al., 2015). Variations of UGTs cause changes in protein structure. Because of this situation, it is thought that these changes affect drug interactions. Structural and confirmational changes caused by variations in the receptor can damage the function of the protein. Thus receptor-drug interactions may be impaired. Patients treated with drugs may show unresponsiveness to the drug due to damage caused by mutations. As a result, drug resistance may develop in patients.

In a study, Huang L. et al. detected that UGT1A1 mutations affected the bioavailability of telmisartan (Huang L. et al., 2019). UGT1A1 encodes the UGT enzyme, which is responsible for metabolizing the drug in the body. Mutations in UGT1A1 affect the coding and production of the enzyme. As a result, the metabolism of the drug also negatively affects this process. Pei Q. et al. also found that UGT1A1 variations affect the pharmacokinetics of telmisartan in Chinese patients (Pei Q. et al., 2017). Shin HJ. Et al. pointed out that Telmisartan pharmacokinetics affected the *UGT1A1* variations in Korean patients. In this study, it was determined that UGT1A1 (rs4148323, rs28934877) variations damage the structure and function of the protein. This may affect the bioavailability and pharmacokinetics of the drug.

In this study, it was observed that the UGT1A1 mutations (rs4148323, rs28934877) are related to telmisartan responsiveness, and these mutations might cause telmisartan resistance. Interactions between telmisartan and wild-type protein and mutant proteins were shown by docking analysis.

5 Conclusion

In this study, it was detected that UGT1A1 (rs4148323, rs28934877) mutations are deleterious. The mutated residue is located in an important domain for protein activity. It was detected that rs4148323 might disturb this function might disturb protein function. rs28934877 is probably damaging to the protein. Protein damage might affect the development of telmisartan resistance in hypertension patients might reduce drug response and complicate the treatment.

Acknowledgments

Authors' contributions: Concept – G.K.K; Design, Supervision, Funding, Materials, Data Collection and/or Processing, Analysis and/or Interpretation, Literature Review, Writing, Critical Review

Conflict of interest disclosure: The author declares that I have no known competing financial interests or personal relationships that could have appeared to influence the work reported in this paper.

Funding: This study received no funding.

Note: This study was presented as a summary paper at the 7th International Congress Applied Science, which was held between Nov. 1, and Nov. 2, 2022 (Kucuk Koprululu G., 2022).

References

BIOVIA, Dassault Systèmes, Discovery Studio, 2021 Cliend, San Diego: Dassault Systèmes, 2022. https://3ds.com/products-services/biovia/products.

Bosma PJ, Van Der Meer IM, Bakker CT, Hofman A, Paul-Abrahamse M, Witteman JC (2003) UGT1A1*28 Allele and coronary heart disease: The Rotterdam study. Clin. Chem. 49(7): 1180–1181

Di YM, Chan E, Wei MQ, Liu JP, & Zhou SF (2009) Prediction of deleterious non-synonymous single-nucleotide polymorphisms of human uridine diphosphate glucuronosyltransferase genes. AAPS Journal, 11(3): 469–480

Ding C, Yang Z, Wang S, Sun F, & Zhan S (2018) The associations of metabolic syndrome with incident hypertension, type 2 diabetes mellitus and chronic kidney disease: a cohort study. Endocrine, 60(2): 282–291

Dutton GJ (1980) Developmental aspects of drug conjugation, with special reference to glucuronidation. Annu Rev Pharmacol Toxicol 18:17–35

Ebner T, Schänzle G, Weber W, Sent U, & Elliott J (2013) In vitro glucuronidation of the angiotensin II receptor antagonist telmisartan in the cat: A comparison with other species. J. Vet. Pharmacol. Ther., 36(2): 154–160

Huang L, Yang L, Huang J, Tan H, Liu S, Kun- Guo C, Pei Q (2019) Effects of UGT1A1 Polymorphism, Gender and Triglyceride on the Pharmacokinetics of Telmisartan in Chinese Patients with Hypertension: A Population Pharmacokinetic Analysis. Eur J Drug Metab Pharmacokinet, 44(6): 797–806

Huang X, Bo Chen F, Dai W, Song L, Tu J, Xu J Zhao S (2018) Prevalence and risk factors associated with hypertension in the Chinese Qiang population. Clin. Exp. Hypertens., 40(5): 427–433

Kılıç M (2016) Uzunçakmak T. Hipertansiyon Hakkındaki Eğitimin Hipertansiyon Kontrolüne Etkisi. Bozok Tıp Dergisi 1(1): 13-9

Kucuk Koprululu G (2022) In Silico Approach for Detection of The Effect of UGT1A1 Polymorphisms on Telmisartan Response. Ed. Guvenmez Korkmaz H. *7th InternationalCongress Applied Science*. ANT Academy. s. 15. Çukurova.

Martinez-Quinones P, McCarthy CG, Watts SW, Klee NS, Komic A, Calmasini FB, Wenceslau CF (2018, September 11). Hypertension induced morphological and physiological changes in cells of the arterial wall. American Journal of Hypertension. Oxford University Press.

Maruo Y, Nishizawa K, Sato H, Sawa H, & Shimada M (2000) Prolonged unconjugated hyperbilirubinemia associated with breast milk and mutations of the bilirubin uridine diphosphate-glucuronosyltransferase gene. Pediatrics 106(5)

Papathanasiou G, Zerva E, Zacharis I, Papandreou M, Papageorgiou E, Tzima C, Evangelou A (2015) Association of High Blood Pressure with Body Mass Index, Smoking and Physical Activity in Healthy Young Adults. Open Cardiovasc. Med. J., 9(1): 5–17

Pei Q, Yang L, Tan HY, Liu SK, Liu Y, Huang L, Yang GP (2017) Effects of genetic variants in UGT1A1, SLCO1B3, ABCB1, ABCC2, ABCG2, ORM1 on PK/PD of telmisartan in Chinese patients with mild to moderate essential hypertension. Int J Clin Pharmacol Ther., 55(8): 659–665

Ritter JK, Chen F, Sheen YY, Tran HM, Kimura S, Yeatman MT, Owens IS (1992) A novel complex locus UGT1 encodes human bilirubin, phenol and other UDP-glucuronosyltransferase isozymes with identical carboxyl termini. J Biol Chem, 267: 3257–3261

Schwertner HA, Vítek L (2008) Gilbert syndrome, UGT1A1*28 allele, and cardiovascular disease risk: Possible protective effects and therapeutic applications of bilirubin. Atherosclerosis. Elsevier Ireland Ltd

Sharpe M, Jarvis B, & Goa KL (2001) Telmisartan: A review of its use in hypertension. Drugs. Adis International Ltd.

Shin HJ, Kim JE, Lim SJ, Seo JE, Kim MH, Hoon OK, Shin JG (2015) Effect of UGT1A1 and UGT1A3 polymorphisms on Pharmacokinetics of Telmisartan in Korean. Clinical Therapeutics, 37(8):87

WHO (2015) http://www.who.int/ Accessed: 14.08.2022

WHO (2015) https://www.who.int/gho/ncd/risk_factors/blood_pressure_prevalence_text/en/ Accessed: 14.08.2022

Yamada A, Maeda K, Ishiguro N, Tsuda Y, Igarashi T, Ebner T, Sugiyama Y (2011) The impact of pharmacogenetics of metabolic enzymes and transporters on the pharmacokinetics of telmisartan in healthy volunteers. Pharmacogenomic, 21(9): 523–530. https://doi.org/10.1097/FPC.0b013e3283482502

Yan Y, Zhang D, Zhou P, Li B, & Huang SY (2017) HDOCK: A web server for protein-protein and protein-DNA/RNA docking based on a hybrid strategy. Nucleic Acids Res. Spec. Publ., 45:365-373

Zhang X, Ao G, Wang Y, Yan W, Wang M, Chen E, Yang, J (2012) Genetic variants and haplotypes of the UGT1A9, 1A7 and 1A1 genes in Chinese Han. Genet. Mol. Biol., 35(2): 428-434

Zhuo ZL, Xian HP, Long Y, Liu C, Sun YY, Ma YT, Zhao XT (2018) Association between cyp2c19 and abcb1 polymorphisms and clopidogrel resistance in clopidogrel-treated chinese patients. Anatol. J. Cardiol., 19(2): 123–129

RESEARCH ARTICLE
Bull Biotechnol (2022) 3(2):45-49
https://doi.org/10.51539/biotech.1180314 Jurnal homepage: www.dergipark.org.tr/biotech

Bulletin of Biotechnology

Serum levels of irisin, adropin and preptin in obese and athletes

Beytullah OZKAYA[1], Davut Sinan KAPLAN[2*], Caner YILDIRIM[2], Hakim CELIK[3], Firat AKCAN[4], Tugba KILIC[2]

[1]*Adiyaman University, Faculty of Medicine , Department of Physiology, Adiyaman, Turkey*
[2]*Gaziantep University, Faculty of Medicine , Department of Physiology, Gaziantep, Turkey*
[3]*Harran University, Faculty of Medicine , Department of Physiology, Sanlıurfa, Turkey*
[4]*Gaziantep University, Department of Sport Sciences, Gaziantep, Turkey*

*Corresponding author : davutsinankaplan@hotmail.com
Orcid No: https://orcid.org/0000-0003-4663-209X

Received : 26/09/2022
Accepted : 23/10/2022

Abstract: The aim of this study is to investigate the endocrine factors thought to play a role in the regulation of energy homeostasis of irisin, adropin and preptin. Our study consists of men between 30-40 years of age including individuals from overweight or obese (n = 25), practicing regular aerobic exercise (n = 25) and sedentary (control, n = 25) groups. Irisin, adropin and preptin levels were studied on blood serum samples prepared using commercially available ELISA kit. The serum irisin level in the obese group was significantly higher than the both exercising and control groups (p <0,05). The serum adropin level in the obese group were significantly lower than control and exercising groups (p <0,05). The serum preptin level in the exercising groups were significantly lower than control (p <0,05). In addition, negative correlation was found between serum adropin and irisin levels (p <0,05). When ROC curves are analyzed, it is seen that high irisin value and low adropin value in obese individuals distinguish obese individuals from other groups with high sensitivity. In this study, serum irisin levels may increase in the obese individuals is due to more muscle activity. In addition, low levels of serum adropin and no change in preptin levels in obese individuals were considered as risk factors in terms of metabolic diseases. As a result, an active lifestyle is suggested to take advantage of the physiological benefits of irisin

Keywords: irisin, adropin, preptin, exercise, obesity

1. Introduction

Obesity, which is defined as excessive accumulation of fat in the body, has been rapidly spreading all over the world and is one of the main factors underlying many diseases (Spiegelman and Korsmeyer 2012). Exercise has been recognized to be helpful to the health, however it is not fully understood yet that how this effect is realized performed (Aydin 2014). Energy homeostasis refers to the metabolic events that involve the storage of energy in the adipose tissue, nutritional behavior, and energy expenditure. It is known that peripheral tissues are involved in energy homeostasis. Therefore, researches have focused on molecules which are effective or considered effective in the endocrine functions of the peripheral tissues, and the energy balance (Aydin, 2014; Irving et al. 2014). Irisin is a thermogenic protein that is primarily muscle originated and providing energy consumption and weight loss by turning white adipose tissue into brown adipose tissue. Irisin has been associated with positive effects on metabolic diseases such as obesity and type 2 diabetes mellitus (T2DM) (Polyzos et al. 2018). Studies on these proteins showed that exercising changes the level of irisin (Kristin et al., 2013). For this reason, we think that it can provide clinical benefit by playing role in cellular communication against obesity.

Adropin is a peptide-structured hormone that is involved in the regulation of lipid metabolism, defined in the liver and brain. Its main functions are to improve glucose tolerance, preventing insulin resistance and dyslipidemia (Aydin, 2014). Adropin is a peptide with effective cardiovascular functions on lipid metabolism. It was shown to be elevated in mice that were fed with high fat diet and were genetically altered obese mice (Kumar et al. 2008). As the result of the study on mice that are lacking adropin, adipose tissues of mice have been increased in significant quantities. It was suggested that it protects endothelial cells by affecting nitric oxide and thus it might be effective in treating cardiovascular disorders (Lovren et al. 2010). Preptin is a peptide that is synthesized from the pancreas, which is effective on glucose metabolism. It has been reported that, preptin is secreted together with insulin from the β cells and increase insulin secretion and be involved in the regulation of glucose metabolism in this way, when blood glucose levels are high (Cheng et al. 2012).

The definition of some beneficial effects of exercise on metabolic diseases led to the hypothesis that myocines

associated with exercise may be related to these effects. Despite the many researches on irisin, the facts that the findings are incompatible with each other, and there is a small number of studies on adropin and preptin are important factors in the design of this study. The aims of this study were 1: to investigated reveal how the new physiological factors, which are irisin, adropin and preptin, are involved in the regulation of energy homeostasis; change in obese, exercising and sedentary individuals, 2: to investigated the relationship between adropin, irisin and preptin levels and whether these parameters change with regularly exercise.

2. Materials and Method

The study started with the approval of Gaziantep University clinical research ethics committee (date: 19.10.2015, protocol number: 2015/271). A total of 75 participants, 25 of whom were overweight or obese, 25 exercising and 25 controls (sedentary), have participated in our study. All of our study groups consisted of male subjects. BMI was used for identifying overweight or obese groups. The BMI can be easily calculated by dividing the body weight in kilograms to the square of the height in meters [body weight/height^2]. BMI should be >25.00 kg/m ^{2} in determining the overweight or obese people that would participate in the study. It was also noted that overweight or obese people included in the study had no health problems and were not implementing a regular exercise program.

The criteria for determining the athletic groups were identified as regular aerobic exercise practicing individuals. It was noted that the exercise protocol was regularly applied over 120 pulses for 3-4 days a week for at least 40 minutes a day. In addition, the exercising group's BMI were considered to be <25 kg/m^2. The criteria for determining the control group (sedentary) was selecting the individuals that do not practice a regular exercise program, that have the BMI <25 kg/m ^{2} and do not have any health problems (cardiovascular disease, renal disease, diabetes mellitus, hypertension, hyperlipidemia and autoimmune disorders).

Blood was taken from the brachial veins of all groups included in the study to 5 ml gelled tubes after an 8 hour overnight fasting. The blood was taken to the gelled flat tubes in order to study the proteins in the serum samples, and they were centrifuged at 4000 rpm for 10 minutes at 4°C. The serum part was separated into ependorfs and stored at -20°C until analysis. After completion of the blood collection procedure, serum samples were studied using commercially available ELISA kits for irisin, adropin and preptin (Catalog Number: CSB-EQ027943HU, CSB-EL007669HU, 201-12-1449 respectively).

SPSS for Windows version 22.0 package program was used for statistical analysis and p < .05 was considered as statistically significant. one way ANOVA and Kruskal–Wallis test was used to compare of the parameters among the control, athletic and obesity groups. Post hoc Tukey was conducted to compare the concentrations of the parameters between the groups. Receiver operator characteristic (ROC) curve analysis was performed to derive cut-off values for the study parameters in irisin and adropin.

3. Results

The mean age was 32.52 ± 4.53 years in the control group, 32.60 ± 3.77 years in the obese group and 31.84 ± 3.66 years in the athlete group. The mean height was 1.74 ± 0.06 m in the control group, 1.75 ± 0.06 m in the obese group and 1.77 ± 0.06 m in the athlete group. There is no statistically significant difference between the groups in terms of age and height (p> 0.05). The mean weight was 71.80 ± 6.45 kg in the control group, 93.50 ± 11.36 in the obese group and 76.14 ± 8.45 kg in the athlete group. The BMI was 23.46 ± 1.20 kg / m2 in the control group, 30.24 ± 2.48 kg / m2 in the obese group and 24.19 ± 2.21 kg / m2 in the athlete group. The weight and BMI data of the obese group were statistically significantly higher than that of both the control and athlete groups (p <0.01) (Table 1).

Table 1. The demographic characteristics of the volunteers participating in the study.

	Control (Mean ± Sd)	***Obese (Mean ± Sd)***	***Athletic (Mean ± Sd)***
Length (m)	1.74±0.06	1.75±0.06	1.77±0.06
Weight (kg)	71.80±6.45	93.50±11.36 #*	76.14±8.45
BMI (kg/m ^{2})	23.46±1.20	30.24±2.48 #*	24.19±2.21
Age	32.52±4.53	32.60±3.77	31.84±3.66

Obese group compared with the control group ($p < 0,05$)
* Obese group compared with the athletic (exercising) group ($p < 0,05$)

There was no statistically significant difference between control and athletic groups in terms of the amount of serum irisin. However, the amount of serum irisin of obese group was found to be statistically significantly higher than both the control and athletic (exercising) groups ($p < 0,05$). The serum adropin level was significantly lower in the obese group than in the control group and the exercising group. No statistically significant difference was found, when control and exercising groups were compared in terms of serum adropin amount ($p > 0,05$). As a result of statistical analysis, there was a significant difference between the control group and the exercising group in terms of serum preptin concentration (p <0.05) (Table 2).

Tablo 2: The amounts of serum irisin, adropin and preptin in the groups.

	Control (Mean ± Sd) (n=25)	***Obese (Mean ± Sd) (n=25)***	***Athletic (Mean ± Sd) (n=25)***
İrisin (ng/ml)	34,87±26,23	60,85±25,30*#	38,60±14,50
Adropin (pg/ml)	2387,54±694,38	1911,06±386,73*#	2296,88±610,55
Preptin (ng/ml)	294,13±240,21	169,70±151,65	152,52±80,45◊

Obese group compared with the control group ($p < 0.05$).
* Obese group compared with the athletic (exercising) group ($p < 0.05$).
◊ Control group compared with the athletic (exercising) group ($p < 0.05$).

We also examined the demographic characteristic and correlation between serum adropine, irisin and preptin levels. Accordingly, when the parameters were analyzed by Weight (kg) and BMI (kg/m^2), a negative correlation between serum adropin and preptin levels, and positive correlation with irisin were detected. There was also a positive relationship between

age and serum irisin level. İn addition to negative correlation between serum adropine and serum irisin was detected (Table 3 and 4).

Table 3: The demographic characteristic and correlation between serum adropine, irisin and preptin levels.

	Adropin (pg/ml)		*İrisin (ng/ml)*		*Preptin (ng/ml)*
	r	p	r	p	r
Age	0,047	0,663	0,267*	0,035	0,035
Weight (kg)	-0,372**	0,002	0,522**	0,000	-0,286*
BMI (kg/m²)	-0,381**	0,002	0,671**	0,000	-0,271*

** Correlation is significant at the 0.01 level (2-tailed).
* Correlation is significant at the 0.05 level (2-tailed).

Table 4: the correlation between serum adropine and irisin levels.

	İrisin (ng/ml)	
	r	**p**
Adropin (pg/ml)	**-0,309***	**0,012**

* Correlation is significant at the 0.05 level (2-tailed).

The values obtained as a result of ROC analysis for serum irisin and adropin are shown in figure 1 and 2. When ROC curves are analyzed, it is seen that high irisin value and low adropin value in obese individuals distinguish obese individuals from other groups with high sensitivity.

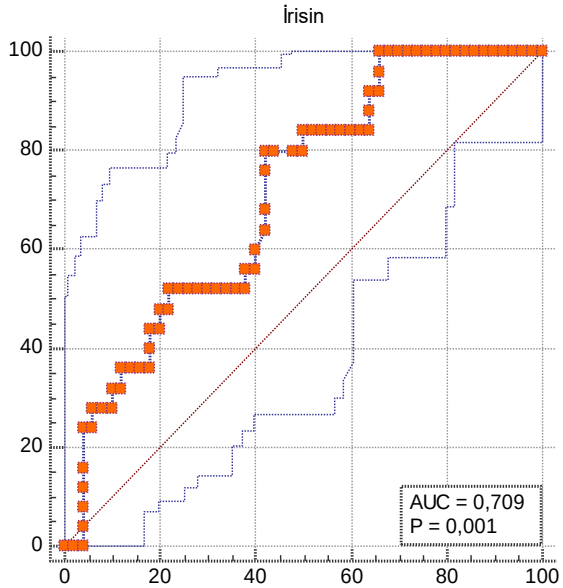

Fig 1. ROC curve belongs irisin values in obesity group is depicted. Area under the curve (AUC):0.709, Sensitivity: 0.80, Specificity:0.58, 95% CI lower border:0.593, 95% CI upper border:0.808.

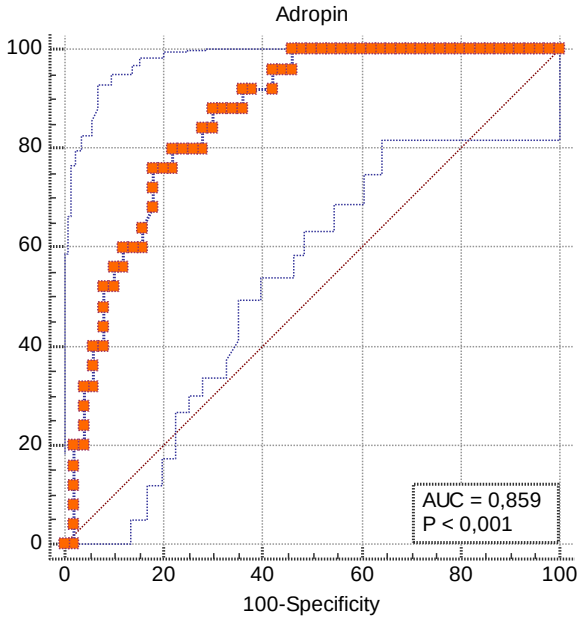

Fig 2 : ROC curve belongs adropin values in obesity group is depicted. Area under the curve (AUC):0.859, Sensitivity: 0.88, Specificity:0.70, 95% CI lower border:0.759, 95% CI upper border:0.928.

4. Discussion

The main findings from this study are as follows. 1: serum irisin levels were significantly higher in the obesity groups than in the control group. 2: serum adropin levels were significantly lower in the obesity groups than in the others. 3: The serum preptin amount decreased significantly with exercise.

Irisin, adropin and preptin are peptides secreted from peripheral tissues involved in regulation of energy homeostasis. The fact that there are uncertainties in the studies on these energy regulators and the lack of sufficient work has laid the ground for investigating this issue. To combat obesity, regular exercise is considered to be one of the most effective methods (Spiegelman and Korsmeyer 2012). Exercise also contributes to individual's continuing a more effective mental and physical life. It also may prevents many chronic illnesses from developing. Furthermore, it is an excellent therapeutic intervention for some types of cancer and control of many diseases such as obesity, type 2 diabetes, dementia, osteoporosis, depression (Aydin 2014; Irving et al. 2014). However, the biological intermediates and the mechanisms by which these therapeutic effects occur are important study areas of today's science.

In this study, consistent with the literature, serum adropine levels were significantly lower in obese individuals than in sedentary and athletic ones. Additionally, there is also only one study evaluating serum adropin level after the exercise. And in that study, the results were similar to our results and it was noted that there was no difference with the control group in terms of the serum adropin level after the exercise. Like other researchers we also think that exercise is not a useful strategy for determining serum adropin levels. Serum adropin

level's being equal with the sedentary after the exercise gives rise to the thought that the amount of adropin increases acutely and drops to normal level after the resting period. The fact that there is no difference in sedentaries in the blood samples taken after exercise program in this study showed that this exercise program did not change the tendency to raise the serum adropin level. Previous studies have revealed a negative association between serum adropin level and BMI. In our study, the data obtained were compatible with the literature and correlation is significant at the 0.01 level (r value -0,381**, p value 0.002). Low serum adropin level has been shown as a marker for various diseases such as; obesity-related dyslipidemia (Butler et al. 2012), nonalcoholic fatty liver disease (Sayin et al. 2014), coronary artery disease (Zhao et al. 2015), acute myocardial infarction (Yu et al. 2014).

Irisin causes increase in total energy expenditure, improvement in glucose tolerance, decrease in fasting insulin, and protection against diet-induced obesity and diabetes in mouse models (Bostrom et al. 2012; Norheim et al. 2014). In studies related to the irisin there has been a mismatch, which is; some researchers have reported an increase in serum irisin level after exercise (Bostrom et al. 2012), while others have shown that there is no increase after chronic exercise, and there is increase only after acute exercise (Huh et al. 2012; Timmons et al. 2012; Pekkala et al. 2013; Norheim et al. 2014). Similarly; our study has also matched with the previous studies (Huh et al. 2012; Timmons et al. 2012; Pekkala et al. 2013; Norheim et al. 2014) and there was no increase in serum irisin level after exercise. Our findings suggest that there is only an increase in muscle activity at the level of irisin, and thus falls back to the sedentary level when the activity decreases in the athletes, i.e. after 8 hours rest period. Previous studies that have examined the association between BMI and serum irisin level have demonstrated a positive correlation. Our results were similar and correlation is significant at the 0.01 level (r value 0,671 **, p value 0,000). This relationship may be due to an induced mechanism to compensate the obesity. (Huh et al. 2012; Stengel et al., 2013). In most, but not all studies in humans, a positive correlation was found between serum irisin with body mass index (BMI) and different anthropometric parameters but has been reported in different results. (Huh et al. 2012; Stengel et al. 2013; Perakakis et al. 2017). In obese people, the circulating irisin concentration was found higher than individuals with normal body mass index (Pardo et al. 2014). The significantly high level of serum irisin found in obese individuals in our study suggests that acute ATP requirement and acute muscle activity to carry body weights of these individuals may be due to much greater activity than sedentaries and athletes. As a result, our study also supports that the level of serum irisin increases after the period when muscle tissue is active, and also supports an active lifestyle to benefit from the physiological benefits of irisin (such as the use of adipose tissue as energy).

Preptin is a peptide structured hormone that is secreted with insulin from β cells, consisting of 34 amino acids, is a derivative of IGF 2 and that increases the insulin secretion (Cheng et al. 2012). Yang et al. compared serum preptin levels in 50 (type 2 diabetes mellitus) T2DM patients, 56 impaired glucose tolerance (IGT) patients, and healthy control group of 54 individuals. Serum preptin level was significantly higher in patients with T2DM compared with IGT and control group. It has been stated that increased levels of preptin in T2DM patients may be due to an increase in preptin secretion or a decrease in preptin metabolism. Moreover, researchers have stated that there is no relationship between BMI and serum preptin level and this result might be linked to preptin and glucose-lipid metabolism and insulin resistance, but it is not linked to the insulin secretion (Yang et al. 2009). Mervat El-Eshmawy et al. compared the serum preptin levels between 100 obese and overweight individuals and healthy control group of 50 individuals. Serum preptin levels were significantly higher in obese and overweighed group than the control group. Researchers have expressed that elevated serum preptin level might be related to the obesity together with the insulin resistance (El-Eshmawy and Abdel Aal 2015). Insulin resistance in obesity leads to an excessive increase of insulin from pancreatic β cells. And in our study, the reason for obese individuals' not having insulin resistance yet is considered as a reason of the fact that serum preptin levels were not changed according to the control group. In our study, serum preptin level in exercise group was significantly more than control group. These data are compatible with the literature (Mohammad et al. 2020).

5. Conclusion

As the result; obese individuals have more acute ATP needs because they have to constantly carry their own body weights. The high level of irisin in obese individuals might be due to the need for this acute ATP. In the exercising group, the level of serum irisin is the same as that of the sedentary group, which might be due to the decrease to the sedentary level as a result of the rest period after meeting the same requirement for ATP. The facts that the level of serum adropin is low in obese individuals and the level of preptin is the same as the control groups, suggest that obese individuals have the suitable background for metabolic diseases such as impaired insulin metabolism in later life if they do not perform BMI control or lose weight. However, further studies are needed for certain reasons, such as; this study has been performed as the first time for some parameters or some of the literature information has been presenting incompatible results.

Acknowledgements

This research did not receive any specific grant from funding agencies in the public, commercial, or not-for-profit sectors.

Conflict of interest disclosure: None

References

Aydin S (2014) Three new players in energy regulation: preptin, adropin and irisin. Peptides 56:94-110. doi:10.1016/j.peptides.2014.03.021

Bostrom P, Wu J, Jedrychowski MP, Korde A, Ye L, Lo JC, Spiegelman BM (2012) A PGC1-alpha-dependent myokine that drives brown-fat-like development of white fat and thermogenesis. Nature 481(7382):463-468. doi:10.1038/nature10777

Butler AA, Tam CS, Stanhope KL, Wolfe BM, Ali MR, O'Keeffe M, Havel PJ (2012) Low circulating adropin concentrations with obesity and aging correlate with risk factors for metabolic disease and increase after gastric bypass surgery in humans. J Clin Endocrinol Metab 97(10):3783-3791. doi:10.1210/jc.2012-2194

Cheng KC, Li YX, Asakawa A, Ushikai M, Kato I, Sato Y, Inui A (2012) Characterization of preptin-induced insulin secretion in pancreatic beta-cells. J Endocrinol 215 (1):43-49. doi:10.1530/JOE-12-0176

El-Eshmawy M, Abdel AI (2015) Relationships between preptin and osteocalcin in obese, overweight, and normal weight adults. Appl Physiol Nutr Metab 40(3):218-222. doi:10.1139/apnm-2014-0338

Huh JY, Panagiotou G, Mougios V, Brinkoetter M, Vamvini MT, Schneider BE, Mantzoros CS (2012) FNDC5 and irisin in humans: I. Predictors of circulating concentrations in serum and plasma and II. mRNA expression and circulating concentrations in response to weight loss and exercise. Metabolism 61(12):1725-1738. doi:10.1016/j.metabol.2012.09.002

Irving BA, Still CD, Argyropoulos G (2014) Does IRISIN Have a BRITE Future as a Therapeutic Agent in Humans? Curr Obes Rep 3:235-241. doi:10.1007/s13679-014-0091-1

Kristin IS, Roeland JWM, Kristy LT, Ding A, Eva BN, Kristen MH, Kathleen RM, Kazuhiro N, Michael FH, Yu-Hua T, Laurie JG (2013) Brown adipose tissue regulates glucose homeostasis and insulin sensitivity. The Journal of Clinical Investigation 123:215-223. doi:10.1172/JCI62308

Kumar KG, Trevaskis JL, Lam DD, Sutton GM, Koza RA, Chouljenko VN, Butler AA (2008) Identification of adropin as a secreted factor linking dietary macronutrient intake with energy homeostasis and lipid metabolism. Cell Metab 8(6):468-481. doi:10.1016/j.cmet.2008.10.011

Lovren F, Pan Y, Quan A, Singh KK, Shukla PC, Gupta M, Verma S (2010) Adropin is a novel regulator of endothelial function. Circulation 122(11 Suppl):185-192. doi:10.1161/CIRCULATIONAHA.109.931782

Mohammad-Rahimi GR, Bijeh N, Rashidlamir A (2020) Effects of exercise training on serum preptin, undercarboxylated osteocalcin and high molecular weight adiponectin in adults with metabolic syndrome. Exp Physiol 105(3):449-459. doi:10.1113/EP088036

Norheim F, Langleite TM, Hjorth M, Holen T, Kielland A, Stadheim HK, Drevon CA (2014) The effects of acute and chronic exercise on PGC-1alpha, irisin and browning of subcutaneous adipose tissue in humans. FEBS J 281(3):739-749. doi:10.1111/febs.12619

Pardo M, Crujeiras AB, Amil M, Aguera Z, Jimenez-Murcia S, Banos R, Casanueva FF (2014) Association of irisin with fat mass, resting energy expenditure, and daily activity in conditions of extreme body mass index. Int J Endocrinol 2014:857270. doi:10.1155/2014/857270

Pekkala S, Wiklund PK, Hulmi JJ, Ahtiainen JP, Horttanainen M, Pollanen E, Cheng S (2013) Are skeletal muscle FNDC5 gene expression and irisin release regulated by exercise and related to health? J Physiol, 591(21):5393-5400. doi:10.1113/jphysiol.2013.263707

Perakakis N, Triantafyllou GA, Fernandez-Real JM, Huh JY, Park KH, Seufert J, Mantzoros CS (2017) Physiology and role of irisin in glucose homeostasis. Nat Rev Endocrinol 13(6):324-337. doi:10.1038/nrendo.2016.221

Polyzos SA, Anastasilakis AD, Efstathiadou ZA, Makras P, Perakakis N, Kountouras J, Mantzoros CS (2018) Irisin in metabolic diseases. Endocrine 59(2):260-274. doi:10.1007/s12020-017-1476-1

Sayin O, Tokgoz Y, Arslan N (2014) Investigation of adropin and leptin levels in pediatric obesity-related nonalcoholic fatty liver disease. J Pediatr Endocrinol Metab 27(5-6):479-484. doi:10.1515/jpem-2013-0296

Spiegelman BM, Korsmeyer SJ (2012) Irisin and the therapeutic benefits of exercise. BMC Proceedings 6(Suppl 3):O23. doi:10.1186/1753-6561-6-s3-o23

Stengel A, Hofmann T, Goebel-Stengel M, Elbelt U, Kobelt P, Klapp BF (2013) Circulating levels of irisin in patients with anorexia nervosa and different stages of obesity-correlation with body mass index. Peptides 39:125-130. doi:10.1016/j.peptides.2012.11.014

Timmons JA, Baar K, Davidsen PK, Atherton PJ (2012) Is irisin a human exercise gene? Nature 488(7413):E9-10 discussion E10-11. doi:10.1038/nature11364

Yang G, Li L, Chen W, Liu H, Boden G, Li K (2009) Circulating preptin levels in normal, impaired glucose tolerance, and type 2 diabetic subjects. Ann Med 41(1):52-56. doi:10.1080/07853890802244142

Yu HY, Zhao P, Wu MC, Liu J, Yin W (2014) Serum adropin levels are decreased in patients with acute myocardial infarction. Regul Pept 190-191:46-49. doi:10.1016/j.regpep.2014.04.001

Zhao LP, Xu WT, Wang L, You T, Chan SP, Zhao X, Yang XJ (2015) Serum adropin level in patients with stable coronary artery disease. Heart Lung Circ 24(10):975-979. doi:10.1016/j.hlc.2015.03.008

RESEARCH ARTICLE
Bull Biotechnol (2022) 3(2):50-55
https://doi.org/10.51539/biotech.1182838 Journal homepage: www.dergipark.org.tr/biotech

Bulletin of Biotechnology

Detection of The Effect of CYP2C19*4 Mutation on Clopidogrel Response by *In Silico* Methods

Gizem Koprululu Kucuk*

*[1]*Department of Radiotherapy, Istanbul Sisli Vocational School, Istanbul, Turkey*

*Corresponding author: gzm0507@gmail.com
Orcid No: https://orcid.org/ 0000-0001-6667-4532

Received : 01/10/2022
Accepted : 23/12/2022

Abstract: Single nucleotide polymorphisms cause amino acid change, and protein structure and function are changed. Thus, the patient improves drug resistance and does not respond to therapy. Clopidogrel is an antiplatelet drug and is used for cardiovascular disease therapy such as heart failure, atherosclerosis, and myocardial infarction.CYP2C19 gene is a CYP450 enzyme and metabolizes clopidogrel. Polymorphism in the CYP2C19 gene causes clopidogrel resistance. A homology modeling study was carried out using the Swiss-Model database and the Chimera program. The selection of models was made with the evaluation of the QMEAN values of the three-dimensional structures. The physicochemical properties of the wild type and CYP2C19*4 mutant type were analyzed by the ExPASy-ProtParam Portal. The effects of the mutation on the protein structure were performed by the HOPE database. The HDock program was used to demonstrate interactions between clopidogrel and wild-type protein and, mutant type protein. Mutation of the residue might disturb this function. This mutation causes the loss of interactions and affects the drug response. In this study, it was shown that Clopidogrel drug interactions between mutant type protein by docking study. Possible drug conformation is designed for the effective treatment of patients carrying the common mutation.

Keywords: Heart failure, drug resistance, clopidogrel, homology modeling, single nucleotide polymorphism (SNP)

1 Introduction

Heart Failure (HF), is a complex syndrome that causes the heart to not be able to send oxygen to the tissues for its metabolic needs, due to insufficient cardiac filling and neurohormonal activation, resulting in shortness of breath, fatigue, and edema (Braunwald E., 2001). The European Society of Cardiology (ESC) defines HF as a cardiac structure and/or functional disorder that causes the heart to not deliver enough oxygen to the tissues for their metabolic needs, despite normal filling pressures (McMurray et al. 2012).

When we look at the frequency of HF seen in the adult population; It is seen that the average is 23 million worldwide, 15 million in European countries, and six million in the United States (Sari et al. 2016; Tokgözoğlu et al. 2018). The prevalence of HF in Turkey according to the results of the Survey on the Prevalence and Determinants of Heart Failure in Turkey (HAPPY) is over two million (Değertekin et al. 2012). Early diagnosis and treatments are the most important to increase the mortality ratio of heart failure patients. When Turkey is compared with other countries, the heart failure patient population is significantly high (McMurray et al. 2012). Heart failure improves at any age but, the incidence of heart failure increases in old age.

Its incidence is increasing in people younger than 65 years of age. HF is the most common cause of hospitalization in individuals over the age of 65. HF is a disease that is very costly to treat due to frequent hospitalizations, causes loss of workforce, and poses a problem for both the patient and society. Therefore, early diagnosis and treatment are important (Sari et al. 2016). The short-term goals of heart failure treatment are to control symptoms and improve quality of life.

Clopidogrel is among the antiplatelet drugs and shows its effect by preventing platelet aggregation (thrombus) that causes blood clotting. Clopidogrel is frequently used in patients with arteriosclerosis, a history of heart attack and stroke, and peripheral vascular disease to prevent thrombus formation in the vessels that cause death by causing conditions such as heart attacks and strokes (Simon et al. 2009). Clopidogrel is a pro-drug which absorbs in the intestine and activates in the liver (Sangkuhl et al.2010).

The CYP2 gene family consists of nine exons and eight introns (Hoffman et al. 2001). CYP2 genes are located on different chromosomes and are arranged in multigene clusters containing one or more subfamilies. The CYP2C19 gene, which is one of the CYP450 enzymes, is localized on the long arm of the 10th chromosome (10q23.3) and consists of 9 exons. CYP2C19 carries polymorphisms that affect the metabolism of drugs related to the treatment of cardiovascular diseases. It is a polymorphic gene (Gandhi et al. 2014). There are 25 different variants of the CYP2C19 allele (Bhat et al. 2015). The active allele (wild type) of the CYP2C19 gene is called CYP2C19*1 (Kim et al. 2010). The CYP2C19*4 key variant is the start codon changing variant A>G (rs28399504). CYP2C19*4 is a rare variant (Scott et al., 2012).

CYP2C19 metabolizes many drugs (Lee et al, 2013). Therefore, CYP2C19 polymorphisms affect the pharmacokinetics of CYP2C19 substrate drugs. Among the many factors that cause differences between individuals in the response to clopidogrel, the most important one is the differences in drug metabolism rates resulting from polymorphism of the CYP2C19 gene (Brown et al. 2018). CYP2C19 enzyme converted the Clopidogrel to its active form in the liver (Mega et al. 2009). Isoforms of hepatic cytochrome P450 (CYP) are responsible for the formation of the active metabolite of Clopidogrel. This process consists of two phases in which CYP2C19, CYP1A2, and CYP2B6 in the first line and CYP2C19, CYP2C9, CYP2B6, and CYP3A in the second line are responsible (Barnette et al. 2019). This active form inhibits a receptor protein which is called P2RY12. This receptor is located on the surface of platelets. The P2RY12 receptor protein provides platelet cluster formation to prevent blood loss. CYP1A2, CYP2B6, CYP2C9, CYP2C19 and CYP3A4 / 5 that are cytochrome P450 enzymes and play a role in clopidogrel metabolism. Studies have shown that CYP3A4, CYP2C9, CYP2C19, and CYP2B6 enzymes metabolize the 2-oxo-clopidogrel and form the active metabolites (Kurihara et al. 2005). Studies showed that a quarter of patients who are treated with clopidogrel have a less-than-normal response to treatment (Shuldiner et al. 2009).

2 Materials and Method

2.1 Homology Modeling Databases

Homology modeling of CYP2C19*4 (rs28399504) is created and Physico-chemical properties are obtained. FASTA format of an amino acid sequence of the CYP2C19 gene is obtained by Uniprot.org and the Gene bank database of National Center for Biotechnology Information, USA, NCBI (https://www.ncbi.nlm.nih.gov/ Accessed: 20.07.2022). Sequence information is arranged according to wild type and mutant type. Sequence with access number P33261 is used in our bioinformatics study for wild type. In the mutant type, Methionine changes to Valine at position 255. The amino acid sequence of the wild type and mutant type is shown in Table 1.

Table 1. The amino acid sequence of wild type and mutant type (M255V) (https://www.ncbi.nlm.nih.gov/ Accessed: 20.07.2022).

Wild Type

MDPFVVLVLCLSCLLLLSIWRQSSGRGKLPPGPTPLPVIGNILQIDIKDVS
KSLTNLSKIYGPVFTLYFGLERMVVLHGYEVVKEALIDLGEEFSGRGHF
PLAERANRGFGIVFSNGKRWKEIRRFSLMTLRNFGMGKRSIEDRVQEE
ARCLVEELRKTKASPCDPTFILGCAPCNVICSIIFQKRFDYKDQQFLNLM
EKLNENIRIVSTPWIQICNNFPTIIDYFPGTHNKLLKNLAFMESDILEKVK
EHQESMDINNPRDFIDCFLIKMEKEKQNQQSEFTIENLVITAADLLGAG
TETTSTTLRYALLLLLKHPEVTAKVQEEIERVIGRNRSPCMQDRGHMP
YTDAVVHEVQRYIDLIPTSLPHAVTCDVKFRNYLIPKGTTILTSLTSVLH
DNKEFPNPEMFDPRHFLDEGGNFKKSNYFMPFSAGKRICVGEGLARME
LFLFLTFILQNFNLKSLIDPKDLDTTPVVNGFASVPPFYQLCFIPV

Mutant Type

MDPFVVLVLCLSCLLLLSIWRQSSGRGKLPPGPTPLPVIGNILQIDIKDVS
KSLTNLSKIYGPVFTLYFGLERMVVLHGYEVVKEALIDLGEEFSGRGHF
PLAERANRGFGIVFSNGKRWKEIRRFSLMTLRNFGMGKRSIEDRVQEE
ARCLVEELRKTKASPCDPTFILGCAPCNVICSIIFQKRFDYKDQQFLNLM
EKLNENIRIVSTPWIQICNNFPTIIDYFPGTHNKLLKNLAFMESDILEKVK
EHQESVDINNPRDFIDCFLIKMEKEKQNQQSEFTIENLVITAADLLGAGT
ETTSTTLRYALLLLLKHPEVTAKVQEEIERVIGRNRSPCMQDRGHMPY
TDAVVHEVQRYIDLIPTSLPHAVTCDVKFRNYLIPKGTTILTSLTSVLHD
NKEFPNPEMFDPRHFLDEGGNFKKSNYFMPFSAGKRICVGEGLARMEL
FLFLTFILQNFNLKSLIDPKDLDTTPVVNGFASVPPFYQLCFIPV

Homology models of CYP2C19 (wild and mutant types) were created with the Swiss Model Program which is an internet-based bioinformatics tool (Waterhouse et al. 2018) and the obtained three-dimensional models were examined with the UCSF Chimera program, which is a visualization tool (Pettersen et al. 2004). A homology modeling study was carried out using the Swiss Model (www.swissmodel.expasy.org, Access date: 25.07.2022; Waterhouse et al, 2018) database and the Chimera program. Wild and mutant-type sequence sets were loaded into the system separately and their three-dimensional structures were obtained. The selection was made with the evaluation of the QMEAN values of the three-dimensional structures. By using UCSF Chimera program tools, the protein structures of the wild type and mutant type were visualized with ribbon display and structural differences of mutant protein were observed.

2.2 Bioinformatic Analysis Of Homology Models

The physicochemical properties of the wild type and CYP2C19*4 mutant type of the CYPC19 gene were analyzed by the ExPASy-ProtParam Portal (Walker 2005). Amino acid number, theoretical pI value, aliphatic index, molecular weight, amino acid composition, negatively and positively charged numbers, and hydrophobicity value were analyzed for each model.

HOPE is a web service that analyzes the structural effect of mutation on the protein sequence. HOPE shows the effects of the mutation on the protein and calculates probable damage of mutation on the protein structure (Venselaar et al. 2010). In this study, it was shown that the effect of CYP2C19*4 on the protein structure by the HOPE database (Venselaar et al. 2010).

2.3 Molecular Docking Study

Docking is a method that involves estimating the conformation and orientation of the ligand structure at a targeted binding site. Docking can also be defined as the determination of the binding mode for a ligand construct to the target protein. Molecular docking studies have an important role in drug discovery. Especially it is so important for drug-resistance therapies. Three-dimensional (3D) structures of ligands and proteins are necessary for docking studies. Docking programs use 3D structures and put in ligands the target region of the protein (Morris et al. 2009).

The HDock server is usually used for drug discovery studies (Yan et al. 2017). HDock which is an atom-based docking method uses a genetic algorithm. Genetic algorithms transfer the energy and geometry information of a newly formed conformation of the molecule to the next conformation and thus they are obtained optimal conformations. In this study, molecular docking of CYP2C19 and clopidogrel was made by HDock, and binding energies of wild and mutant types were calculated.

3 Results

The amino acid sequence format which is used as a basis in bioinformatics studies was created based on the NCBI-P33261 accession number sequence (https://www.ncbi.nlm.nih.gov/ Accessed: 20.07.2022). Three-dimensional structures were obtained by using CYP2C19 wild and mutant type sequence sets, for which homology modeling was performed using the Swiss-Model database and the Chimera program (Waterhouse et al. 2018; Pettersen et al. 2004). CYP2C19 wild and mutant-type ribbon structures were shown in Figure 1.

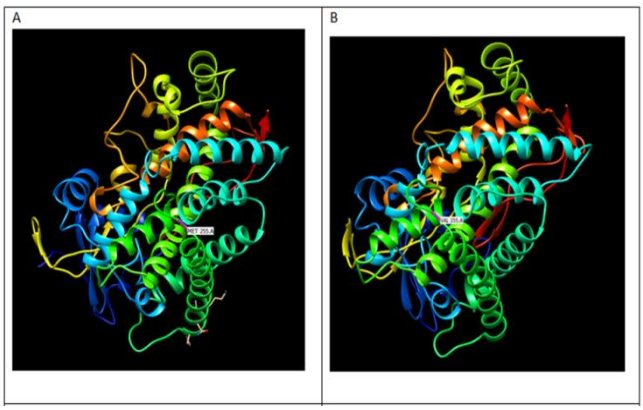

Figure 1. A: CYP2C19 wild-type ribbon structure, B: CYP2C19*4 mutant-type ribbon structure (Pettersen et al. 2004).

Each amino acid has its specific size, charge, and hydrophobicity value. CYP2C19 wild and mutant-type hydrophobicity were shown in Figure 2 as hydrophobic surfaces by the Chimera program (Pettersen et al. 2004).

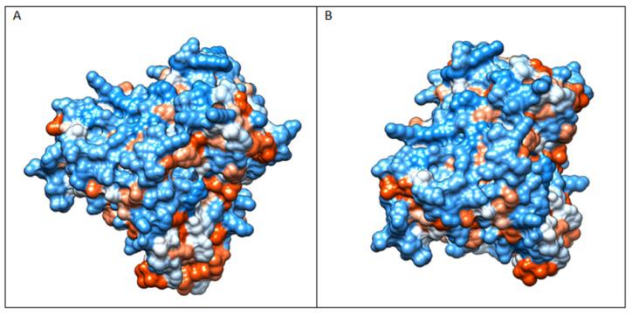

Figure 2. A: CYP2C19 gene wild type hydrophobic structure, B: CYP2C19 mutant type hydrophobic structure (Pettersen et al. 2004).

Schematic structures of the wild (left) and the mutant (right) amino acids were shown in Figure 3.

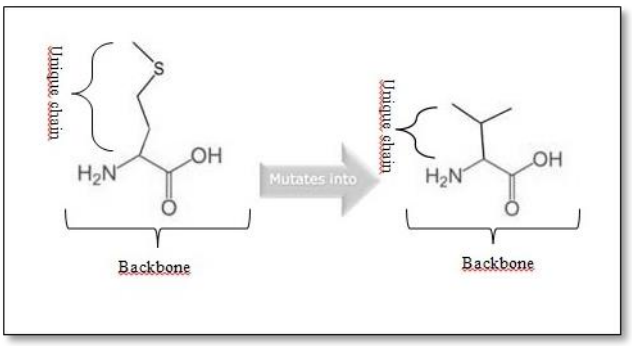

Figure 3. The wild (left) and the mutant (right) amino acid schematic structures (Venselaar et al. 2010).

The original wild-type residue and newly introduced mutant residue often differ in these properties. The mutant residue is smaller than the wild-type residue. The mutated residue is located in a domain that is important for the binding of other molecules. Mutation of the residue might disturb this function.

The amino acid change was shown in Figure 4. The side chains of both the wild-type and the mutant residue were shown in the figure with labels.

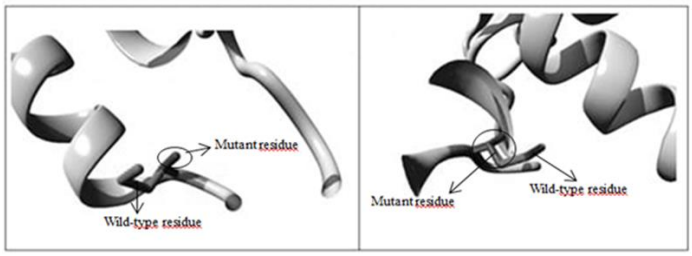

Figure 4. Close-up of the mutation (Venselaar et al. 2010).

We observed that the mutant residue is smaller, this situation might lead to a loss of interactions. It is possible that the mutant residue affects protein activity and function as it is located at the binding site.

The grand average of the hydropathicity (GRAVY) index shows the solubility of the proteins (Table 2). If it is a positive charge, it means that hydrophobic, and if it is negative, it means hydrophilic (Chang et al. 2013). While wild-type protein is hydrophilic, mutant-type is hydrophobic.

Table 2. Physicochemical properties of wild and mutant proteins (Walker 2005).

CYP2C19 Wild Type	**CY2C19*4 Mutant Type**
Number of amino acids: 490	**Number of amino acids:** 490
Molecular weight: 55931.06	**Molecular weight:** 55899.00
Theoretical pI: 7.11	**Theoretical pI:** 7.11
Amino acid composition:	Ala (A) 17 3.5%
Ala (A) 17 3.5%	Arg (R) 27 5.5%
Arg (R) 27 5.5%	Asn (N) 26 5.3%
Asn (N) 26 5.3%	Asp (D) 24 4.9%
Asp (D) 24 4.9%	Cys (C) 13 2.7%
Cys (C) 13 2.7%	Gln (Q) 16 3.3%
Gln (Q) 16 3.3%	Glu (E) 33 6.7%
Glu (E) 33 6.7%	Gly (G) 28 5.7%
Gly (G) 28 5.7%	His (H) 10 2.0%
His (H) 10 2.0%	Ile (I) 35 7.1%
Ile (I) 35 7.1%	Leu (L) 56 11.4%
Leu (L) 56 11.4%	Lys (K) 30 6.1%
Lys (K) 30 6.1%	Met (M) 12 2.4%
Met (M) 13 2.7%	Phe (F) 33 6.7%
Phe (F) 33 6.7%	Pro (P) 30 6.1%
Pro (P) 30 6.1%	Ser (S) 26 5.3%
Ser (S) 26 5.3%	Thr (T) 27 5.5%
Thr (T) 27 5.5%	Trp (W) 3 0.6%
Trp (W) 3 0.6%	Tyr (Y) 11 2.2%
Tyr (Y) 11 2.2%	Val (V) 33 6.7%
Val (V) 32 6.5%	Pyl (O) 0 0.0%
Pyl (O) 0 0.0%	Sec (U) 0 0.0%
Sec (U) 0 0.0%	(B) 0 0.0%
(B) 0 0.0%	(Z) 0 0.0%
(Z) 0 0.0%	(X) 0 0.0%
(X) 0 0.0%	**Total number of negatively charged residues (Asp + Glu):** 57
Total number of negatively charged residues (Asp + Glu): 57	**Total number of positively charged residues (Arg + Lys):** 57
Total number of positively charged residues (Arg + Lys): 57	**Atomic composition:**
Atomic composition:	Carbon C 2529
Carbon C 2529	Hydrogen H 3986
Hydrogen H 3986	Nitrogen N 666
Nitrogen N 666	Oxygen O 711
Oxygen O 711	Sulfur S 25
Sulfur S 26	**Formula:** C2529H3986N666O711S25
Formula: C2529H3986N666O711S26	**Total number of atoms:** 7917
Total number of atoms: 7918	**Instability index:**
Instability index:	The instability index (II) is computed to be 43.37
The instability index (II) is computed to be 43.68	This classifies the protein as unstable.
This classifies the protein as unstable.	**Aliphatic index:** 95.43
Aliphatic index: 94.84	**Grand average of hydropathicity (GRAVY):** -0.093
Grand average of hydropathicity (GRAVY): -0.098	

Molecular docking interaction of Clopidogrel and CYP2C19 wild and mutant types was carried out using the HDock server. HDock is used Bioinformatics-based methods to predict the structure and generate interactions (Yan et al. 2017). Clopidogrel docking results were shown in Figure 5.

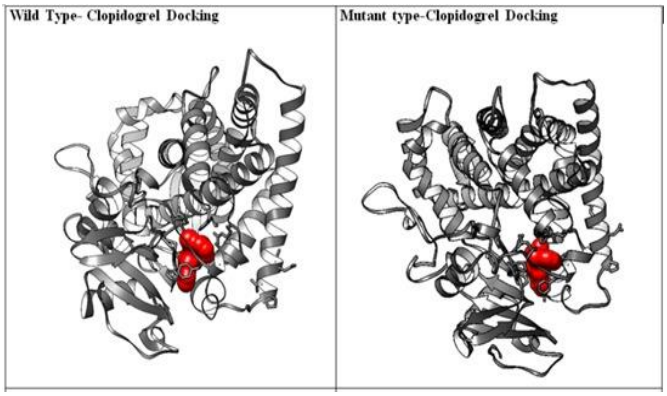

Figure 5. Molecular docking interaction of Clopidogrel and CYP2C19 wild and mutant type (Yan et al. 2017).

4 Discussion

The United States Food and Drug Administration (FDA) gave some warnings on clopidogrel metabolism and the CYP2C19 gene in 2017 (FDA, 2017). It was reported that some patients metabolized clopidogrel poorly and developed drug resistance. Clopidogrel activity would decrease in these patients. Shuldiner et al. determined the effect of 13 polymorphisms located near the CYP2C18-2C19-2C9-2C8 gene region on the response to clopidogrel treatment. The CYP2C19*2 genotype is detected in approximately 12% of individuals with variable responses to clopidogrel (Shuldiner et al. 2009).

Liu Y. et al. detected that the loss of function of the CYP2C19 gene causes cardiovascular system diseases in Chinese patients (Liu et al. 2013). Siller-Matula JM et al. explained that the loss of function alleles (*2, *3, *4, *5, *6, *7, and *8) were responsible for the cardiovascular diseases risk (Siller-Matula et al. 2013). Pettersen et al. detected that CYP2C19*2 carriers were observed to have higher platelet activity than non-carriers (Pettersen et al. 2004). Zhuo ZL et al. found that the CYP2C19 mutant allele was significantly associated with clopidogrel responsiveness and explained that CYP2C19*4 and CYP2C19*5 are associated with clopidogrel resistance in the Caucasian population (Zhuo et al. 2018). Jeong YH. et al. showed that CYP2C19*2 and *3 affects clopidogrel response, the pharmacodynamics of clopidogrel, and cardiovascular events (Jeong YH. et al. 2011). Holmes DR. et al. detected that CYP2C19*4, CYP2C19*5, CYP2C19*6, CYP2C19*7, and CYP2C19*8 have low clopidogrel metabolism (Holmes DR. et al. 2010).

In this study, it was observed that the CYP2C19*4 mutation is related to clopidogrel responsiveness, and this mutation might cause clopidogrel resistance. Interactions between clopidogrel and mutant protein and wild-type protein were shown by docking analysis.

5 Conclusion

In this study, it was detected that CYP2C19*4 (rs28399504) mutation might disturb protein function and activity. The interactions between clopidogrel and wild and mutant-type proteins were observed. It was thought that CYP2C19*4 (rs28399504) mutation might affect the development of clopidogrel resistance in heart failure patients and also it might reduce drug response and complicate the treatment.

Acknowledgments

Author Contributions: Concept – G.K.K; Design, Supervision, Funding, Materials, Data Collection and/or Processing, Analysis and/or Interpretation, Literature Review, Writing, Critical Review

Declaration of Interests: The author declares that I have no known competing financial interests or personal relationships that could have appeared to influence the work reported in this paper.

Funding: This study received no funding.

Note: This study was presented as a summary paper at the 5th International Eurasian Conference on Biological and Chemical Sciences, which was held between Nov. 23, and Nov. 25, 2022 (Kucuk Koprululu G., 2022).

7 References

Barnette DA, Davis MA, Flynn N, Pidugu AS, Swamidass SJ, & Miller GP. (2019). Comprehensive kinetic and modeling analyses revealed CYP2C9 and 3A4 determine terbinafine metabolic clearance and bioactivation. Biochem. Pharmacol. 170.

Bhat IA, Pandith AA, Yaqoob I, Faheem S, Hafeez I, Beig JR, et al., (2015) Genetic Determinants of CYP2C19 Gene* 2 and* 3 Loss of Function Alleles and Response to Anti Platelet Therapy (Clopidogrel) and Cardiovascular Events (A Study in Kashmir, North India), Biol Med 7(5):1.

Braunwald E (2001) Congestive Heart Failure: A Half-Century Perspective, Eur. Heart J 22: 825-836.

Brown SA, Pereira N, (2018) Pharmacogenomic impact of CYP2C19 variation on clopidogrel therapy in precision cardiovascular medicine, J Pers Med 8(1):8.

Chang KY, Yang JR, (2013) Analysis and Prediction of Highly Effective Antiviral Peptides Based on Random Forests, PLoS ONE 8(8). https://doi.org/10.1371/journal.pone.0070166

Değertekin M, Erol Ç, Ergene O, et al., (2012) Heart failure prevalence and predictors in Turkey: HAPPY study, Arch Turk Soc Cardiol 40: 298-308.

FDA (2017) Drug Safety Communication: Reduced effectiveness of Plavix (clopidogrel) in patients who are poor metabolizers of the drug.

Gandhi S, Zile B, Tan MK, Saranu J, Bucci C, Yan AT, et al., (2014) Increased uptake of guideline-recommended oral antiplatelet therapy: insights from the Canadian Acute Coronary Syndrome Reflective, Can J Cardiol 30:1725– 1731.

Hoffman SM, Nelson DR., Keeney DS, (2001) Organization, structure and evolution of the CYP2 gene cluster on human chromosome 19. Pharmacogenet. Genomics 11:687–698.

Holmes DR Jr, Dehmer GJ, Kaul S, Leifer D, O'Gara PT, Stein MC. (2010). ACCF/AHA clopidogrel clinical alert: approaches to the FDA "boxed warning": a report of the American College of Cardiology Foundation Task Force on clinical expert consensus documents and the American Heart Association endorsed by the Society for Cardiovascular Angiography and Interventions and the Society of Thoracic Surgeons. J Am Coll Cardiol.56(4):321-341.

https://www.ncbi.nlm.nih.gov/ Access date: 20.07.2022

https://www.swissmodel.expasy.org, Accessed: 25.07.2022.

Jeong YH, Tantry US, Kim IS, Koh JS, Kwon TJ, Park Y, et al. (2011). Effect of CYP2C19 *2 and *23 loss-of-function alleles on platelet reactivity and adverse clinical events in East Asian acute myocardial infarction survivors treated with clopidogrel and aspirin. Circul. 4(6): 585–594.

Kim KA, Song WK, Kim KR, Park JY, (2010) Assessment of CYP2C19 genetic polymorphisms in a Korean population using a simultaneous multiplex pyrosequencing method to simultaneously detect the CYP2C19* 2, CYP2C19* 3, and CYP2C19* 17 alleles. J Clin Pharm Ther 35(6): 697-703.

Kucuk Koprululu G (2022) Detection of The Effect of CYP2C19*4 Mutation on Clopidogrel Response by In Silico Methods Ed. Dogan M. 5th International Eurasian Conference Biological and Chemical Sciences s. 57. Ankara.

Kurihara AHK, Kazui M, Ishizuka T, Farid NA, Ikeda T (2005) In vitro metabolism of antiplatelet agent clopidogrel: cytochrome P450 isoforms responsible for two oxidation steps involved in the active metabolite formation, Drug Metab Rev 37:99.

Lee SJ, (2013). Clinical application of CYP2C19 pharmacogenetics toward more personalized medicine. Front. Genet. https://doi.org/10.3389/fgene.2012.00318

Liu Y, Liu N, Li W, Shao H, Zhi H, Li J, (2013) Relationship of CYP2C19* 2 and CYP2C19* 3 gene polymorphism with clopidogrel response variability and recurrent cardiovascular events in Chinese patients undergoing percutaneous coronary intervention, J Pharmacol 91(3-4): 165-172.

McMurray JJ, Adamopoulos S, Anker SD, Auricchio A, Böhm M, Dickstein K, et al., (2012) Heart Failure Association. ESC Guidelines for the diagnosis and treatment of acute and chronic heart failure, Turk Kardiyol Dern Ars 40:77–137.

Mega JL, Close SL, Wiviott SD, Shen L, Hockett RD, Brandt JT, et al., (2009) Cytochrome p-450 polymorphisms and response to clopidogrel, N Engl J Med 360:354–362.

Morris GM, Huey R, Lindstrom W, Sanner MF, Belew RK, Goodsell DS, et al., (2009) AutoDock4 and AutoDockTools4: Automated docking with selective receptor flexibility, J. Comput. Chem 30(16):2785–2791.

Pettersen EF, Goddard TD, Huang CC, Couch GS, Greenblatt DM, Meng EC, Ferrin TE, (2004) UCSF Chimera—a visualization system for exploratory research and analysis. J Comput Chem 25(13):1605-1612.

Sangkuhl K, Klein TE, Altman RB, (2010) Clopidogrel pathway, Pharmacogenet. Genomics 20(7): 463.

Sari I, Çavuşoğlu Y, Temizhan A, Yilmaz MB, Eren M, (2016) ESC and ACC/AHA/HFSA heart failure guideline updates: Changes, similarities, differences, and unresolved issues, Turk Kardiyol Dern Ars 44(8):625–36.

Scott, SA, Martis S, Peter I, Kasai Y, Kornreich R, & Desnick RJ. (2012). Identification of CYP2C19*4B: Pharmacogenetic implications for drug metabolism including clopidogrel responsiveness. Pharmacogenomics 12(4): 297–305.

Shuldiner AR, O'Connell JR, Bliden KP, Gandhi A, Ryan K, Horenstein RB, Pollin TI, (2009) Association of cytochrome P450 2C19 genotype with the antiplatelet effect and clinical efficacy of clopidogrel therapy, Jama 302(8): 849-857.

Siller-Matula JM, Trenk D, Schror K, Gawaz M, Kristensen SD, Storey RF et al., (2013) Response variability to P2Y12 receptor inhibitors: expectations and reality. JACC Cardiovasc Interv 6(11):1111-1128.

Simon T, Verstuyft C, Mary-Krause M, Quteineh L, Drouet E, Méneveau N, et al., (2009) Genetic determinants of response to clopidogrel and cardiovascular events, N Engl J Med 360: 363–375.

Tokgözoğlu L, Yılmaz MB, Abacı A, Altay H, Atalar E, Aydoğdu S, et al. (2018) Türkiye'de kalp yetersizliği yol haritası

Venselaar H, te Beek TAH, Kuipers RKP, Hekkelman ML, Vriend G, (2010) Protein structure analysis of mutations causing inheritable diseases, An e-Science approach with life scientist friendly interfaces. BMC Bioinform, https://doi.org/10.1186/1471-2105-11-548

Walker JM, (2005): The Proteomics Protocols Handbook, Humana

Waterhouse A, Bertoni M, Bienert S, Studer G, Tauriello G, Gumienny R, Heer FT, de Beer TAP, Rempfer C, Bordoli L, Lepore R, Schwede T, (2018) SWISS-MODEL: homology modelling of protein structures and complexes, Nucleic Acids Res 46: 296-303.

Yan Y, Tao H, He J, Huang S-Y, (2020) The HDOCK server for integrated protein-protein docking, Nat Protoc 15(5):1829-1852

doi: https://doi.org/10.1038/s41596-020-0312-x.

Zhuo ZL, Xian HP, Long Y, Liu C, Sun YY, Ma YT, et al., (2018) Association between cyp2c19 and abcb1 polymorphisms and clopidogrel resistance in clopidogrel-treated chinese patients, Anatol J Cardiol 19(2):123–129.